APPLICATION OF REMOTE SENSING AND GEOGRAPHIC INFORMATION SYSTEMS FOR GOLD POTENTIAL MAPPING IN BIRIM NORTH DISTRICT OF EASTERN REGION OF GHANA.

By

Clement Kwang BSc. Geomatic Engineering (Hons.)

A Thesis submitted to the Department of Geomatic Engineering, Kwame Nkrumah University of Science and Technology in partial fulfilment of the requirements for the degree of

MASTER OF SCIENCE

Geomatic Engineering Department, College of Engineering

August, 2013

DECLARATION

I hereby declare that this submission is my own work towards the MSc. and that, to the best of my knowledge, it contains no materials previously published by another person nor material which has been accepted for the award of any other degree of the University, except where due acknowledgement has been made in the text.

Clement Kwang, 20129871 .... 19/09/2013

Students Name & ID Signature Date

Certified by

Dr. Edward Matthew Osei Jnr 19/09/2013

Supervisor's Name Signature Date

Certified by

Rev. John Ayer 19/09/2013

Head of Department Signature Date

Abstract

Remote Sensing and Geographic Information System (GIS) have played an active role in mineral exploration by helping in the identification or discovery of new gold deposits in most parts of the world such as Spain, Nova Scotia (Canada) and Egypt. Different authors have used Remote Sensing and GIS in exploring minerals deposits. Birim North District of the Eastern Region of Ghana is one of the gold-mineralized districts but there is no gold potential map covering the whole district. This research work was aimed at producing a gold potential map covering the whole of Birim North District through the use of Remote Sensing and GIS technique. The Landsat Enhanced Thematic Mapper (ETM+) image of the Birim North was processed by applying the clay-mineral ratio (Band 5 to Band 7) and the principal component analysis. The result was further processed to obtain the alteration map of Birim North District which represented the altered rocks associated with gold- mineralization. The Aeromagnetic image of the same area was enhanced by using the Edge Detection Directional Filter and digitized manually on-screen to produce the lineament map of Birim North District. The results obtained from the Remote Sensing processes were integrated into GIS environment with other geospatial datasets such as the soil geochemical data and geophysical data. The Arc-weight of evidence was used as the spatial data integration model in the prediction of the potential gold areas. A total of 250 known gold deposits were used, 180 were used as training samples and 70 were used for the validation. The results obtained from the research work indicated that the best predictors of the new gold deposits were the soil geochemical data, geophysical data and the lineament. The alteration was the least predictor. The gold potential map demarcates 158 km^2 (i.e., 32%) of the total of 497 km^2 as favourable for the occurences of the gold deposits within the study area. The gold potential map

also has a success rate of 88% (i.e, the percentage of the training deposits or points in the predicted favourable gold deposits zones) and a prediction rate of 83% (i.e, the percentage of the validation deposits or points in the predicted favourable gold deposits areas). Many of the mining communities and Newmont Ghana Gold limited mine area were found in the areas associated with relative higher posterior probabilities.

Table of Contents

List of Tables

List of Figures

List of Abbreviation

ASTER……..Advanced Spaceborne Thermal Emission and Reflection Radiometer

C……………Contrast

ETM+………..Enhanced Thematic Mapper Plus

GIS…………. Geographic Information System

IR…………… Infrared

NIR…………..Near Infrared

PCA………… Principal Component Analysis

RGB………… Red Green Blue

SWIR…………Short Wave Infrared

TM……………Thematic Mapper

W+……………Positive Weight

W-……………Negative Weight

WofE…………Weight of Evidence

WRS…………Worldwide Reference System

Acknowledgement

I am very grateful to the Almighty God for His blessings; guidance, strength and gift of life granted me throughout my study.

I wish to express my appreciation and gratitude to my supervisor, Dr. E. M. Osei Jnr. for his fatherly care, constructive criticism and helpful advice throughout my study. All lecturers and the staff of Geomatic Engineering Department, I say thank you for your contributions.

Special thanks go to Eric Twene, Ebenezer Asare, Seth Assam and Eugene Adubofour for their support, contribution and dedication to the success of this project work. I say may the good Lord bless you all.

Many thanks also go to my course mates and Michael Appiah who provided support in one way or the other to me.

Finally to my family and Alice Kwartemaa, I owe you many thanks for the support granted me in times of difficulties and the words of encouragement offered throughout my studies.

CHAPTER ONE

1.0 INTRODUCTION

1.1 Background Information

The prospecting of metals and materials needed to sustain human lives begun since ancient times. The value placed on these metals such as gold made prospectors travel in search of these metals. The specific properties of gold such as its malleability, ductility, good conduction of heat and its inactive nature to air, heat, moisture and most solvents placed its price in a better position in the world market. This has resulted in the establishment of various gold mining companies in the country.

The mineral prospecting companies and the mining companies use different datasets to search for new mineral deposits. These data may be from Geologic map, Remote Sensing, Geophysical and Geochemical operations. In the past these data were integrated and managed in analogical way by overlapping different layers of information in attempt to recognize relationship between layers. These datasets can now be managed and integrated into Geographic Information System (GIS) to deliver a meaningful output or result (Rajesh, 2004). The application of GIS in the field of mineral exploration is based on the fact that the fundamental principles involved in the formation of ore deposits are too complex to be approximated by using analytical mathematical models (Bonham-Carter, 1991). GIS, however, allow for more effective integration and analysis of large number of georeferenced spatial data with different attributes and format in selecting the best sites of mineral deposits (Rajesh, 2004).

The commercial mineral exploration companies are constantly on the lookout for new technologies that can help them identify mineral reserves in a quicker time frame and at a reduced cost. One of such technologies, which are being currently used in the prospecting of mineral deposits, is by using GIS and Remote Sensing technique.

Since the launch of the Landsat in 1972, mineral exploration has been successfully carried out using Remote Sensing and has proven its applications in extracting and locating alteration zones that are related to gold deposits (Gabr et al., 2010). Most countries across the world have used Remote Sensing and GIS in exploring their mineral deposits and some of these nations are Sudan, Egypt and Argentina. The sensors of these satellites can register the spectral signatures and other geologic features related to the mineral deposits.

Gold is one of the minerals that have been explored through the use of Remote Sensing imagery (Rejash, 2004). Although gold cannot be detected directly by any remote sensor, the presence of minerals which were formed in association with gold can be detected based on their spectral signatures. These minerals, called clay minerals, are characteristic of hydrothermal alteration and have diagnostic spectral signatures mostly in the shortwave infrared portion of the electromagnetic spectrum. These signatures can be used to locate areas most favourable to the occurrence of gold deposits (Torres, 2007).

According to Legg (1994), Remote Sensing data often constitutes an important part of the dataset used in GIS because of its intrinsic digital nature, and because it can be used as base map over which to overlay other data. Remote Sensing data provide important help when carrying out exploration activities in remote areas where there is poor or no updated topographic maps. By applying the right image processing techniques, Remote Sensing data can be a useful source of information when exploring for gold deposits.

In addition, if the bands of the satellite imagery are ratioed, they can give a general idea of geologic characteristics, like the presence of clay minerals or the position and the direction of main structure. Remote Sensing has also played an important role in lithogic, structural and alteration mapping. In addition to these, the use of hyperspectral Remote Sensing in mineral resource mapping is important. Hyperspectral data can help identification and thematically map regions of exploration interest by using the distinct absorption features of most minerals (Rajesh, 2004). For the past 36 years, moderate –resolution Remote Sensing image have been used by geologists to create both regional and local geologic maps and has also played an important role in the discovery of new occurrence of oil, gold and other resources (Torres, 2007).

Sabins (1999) indicated that there are two main general approaches for using Remote Sensing in mineral exploration. The first approach is to map geology and structures at regional and local scale. The second approach is to use the hydrothermal alteration that is associated with the mineral deposits. In addition, topographic data in the form of digital elevation can be combined with Remote Sensing data to map geologic features indicative of mineralisation of the type sought (Rokos et al., 2000).

1.2 Problem Statement

This research work focused on the application of Remote Sensing and GIS in mineral exploration of gold deposits in the Birim North District of the Eastern Region of Ghana.

Gold potential map or gold resource map has play an important role in mining since it helps the mining company to focus its exploration efforts over the most favourable and prospective areas, thereby increasing the possibility of mineral discoveries at both reduced cost and limited time frame but there is no such potential map covering the whole of the study area.

According to Boleneus el al., (2001), mineral potential map can be employed for the planning of land use by predicting future exploration activities. However, these mineral potential maps have been produced based on a rigorous field prospecting method. The processes, however, used in the exploration of these minerals are complex and therefore needs both analysis and integration of multithematic exploration information in order to discover a mineral deposit. The expensive nature of field prospecting, the large workforce, the time, and the numerous operations that prospectors have to go through before a mineral is discovered may be attributed to the lack of mineral potential maps for the whole area.

1.3 Main Objective

The main objective of this study is to contribute to the general body of knowledge and research work by producing a gold potential map of Birim North District of Eastern Region.

1.4 Specific Objectives

In order to achieve the main objective of this study, the research is being aimed at addressing the following specific objectives:

1. To study the rocks types from the geologic map of Birim North District.
2. To extract lineament from the Remote Sensing data.

3. To perform band ratio on the Remote Sensing imagery in order to identify and map out minerals associated with gold mineralization.
4. To integrate various datasets into GIS environment for analysis such as calculating weights for each predictive map (evidential theme) and combining the evidential theme to predict the potential gold deposit.

1.5 Research Questions

This research work tends to address the following questions:

A. How can gold potential areas in the Birim North be mapped?
B. How can lineament be extracted from Remote Sensing data?
C. How can hydrothermal alteration or minerals associated with gold mineralization be mapped from Remote Sensing data?
D. What types of rock are associated with gold mineralization within the study area?
E. What are the best predictors in the integration of the various exploratory datasets?
F. What is the total area of gold mineralization within the study area?

1.6 Justification

For the past years, numerous exploration activities required before a mineral is discovered was tedious and expensive. The time and workforce required for drilling and other activities were some of the problems faced by the exploration companies. With the advancement of technology, newer and quicker method of exploring minerals was developed through the application of Remote Sensing and GIS. This method saves time and is of a reduced cost. The gold potential map produced will be an important asset to mining companies, the mineral commission and the nation as a whole.

1.7 Structure of the Project Work

Chapter one of this thesis deals with the introduction of the project work. It includes the background information of the research work, the problem definition, the objective of the research work, justification and the structure of the thesis. **Chapter two** also reviews the relevant literature about the project work and also some of the previous work done by various authors in this research area. It further highlights on spectral signature of minerals and rocks, hydrothermal alteration, lineament, band ratio, Landsat Enhanced Thematic Mapper (ETM+), mineral potential mapping and the weight of evidence. **Chapter three** talks of information about the study area which includes location and size of the study area, relief and drainage, climate and vegetation and geology and soil types, the materials and methods that are used so that the objective of the project work may be achieved. **Chapter four** displays the results obtained from the materials and method used. It further discusses the results obtained from the Remote Sensing processes and other processes that were performed in order to achieve the desire objective. **Chapter five** finally highlights on the conclusion and recommendation.

CHAPTER TWO

2.0 LITERATURE REVIEW

2.1 Introduction

For the past four decades, there has being an intensive increase in the use of remotely sensed data for various types of resource, environmental, and urban studies. The evolving capability of GIS makes it possible for computer systems to handle geospatial data in a more efficient and effective way. Remote Sensing systems, particularly those deployed on satellites, provide a repetitive and consistent view of the earth, which is invaluable to monitoring short-term and long-term changes and the impact of human activities.

Qihao (2010) defined Remote Sensing as the science and technology of acquiring information about the earth's surface (i.e., land and ocean) and atmosphere using sensors on board airborne (e.g., aircraft or balloons) or space borne (e.g., satellites and space shuttles) platforms. Depending on the scope, Remote Sensing may be broken down into (1) Satellite Remote Sensing (when satellite platforms are used), (2) Photography and Photogrammetry (when photographs are used to capture visible light), (3) Thermal Remote Sensing (when the thermal infrared portion of the spectrum is used), (4) Radar Remote Sensing (when microwave wavelengths are used), and (5) LiDAR Remote Sensing (when laser pulses are transmitted toward the ground and the distance between the sensor and the ground is measured based on the return time of each pulse).

GIS are a powerful set of computer-based tools used to collect, store, manipulate, analyse and display spatially referenced information (Burrough and McDonnell, 1998).

2.2 Previous Work on Mineral Exploration

Chica-Olmo et al. (2002) applied Remote Sensing techniques and spatial data analysis through GIS in a mineral exploration context to identify gold-rich potential areas in southern eastern Spain. The Remote Sensing results were integrated, in conjunction with existing maps and data from mineral exploration surveys, into the GIS as vector or raster layers. The result confirmed the usefulness of this integrated methodological approach as an effective tool to assess mineral potential in the studied region.

Chandrasekar et al. (2011) investigated heavy-mineral deposits using multispectral satellite data to map out the mineral deposits in South Tamil Nadu Coast of India. They mapped out minerals which show significant variation in reflectance at different spectral bands. The study has opened up new areas for inland heavy mineral exploitation and lead to eco-friendly exploitation of natural resources along the study area. It also illustrated the high potential of multispectral satellite data for exploration and mapping of mineral resources.

Bonham-Carter et al. (1988) used GIS to integrate a variety of datasets such as geological map, airborne geophysical survey data, geochemistry of lake-sediment samples and mineral occurrence data to create a map showing areas favourable for gold mineralisation in Nova Scotia. Their map confirmed that major known gold districts coincided with area of high probability. Also, several new areas of high probability were discovered by their model or map.

Akhavi and Raymond (2001) carried a similar work by using Radarsat S2, geological, geophysical and stream sediment mineral concentration data layer to create a mineral resource map of the North-Central Nova Scotia. They integrated the S2 mode Radarsat imagery with digital geological, geophysical and stream sediment mineral data layers by utilising GIS and image analysis software packages. Their result contributed to a better understanding of the geological nature of Central Nova Scotia and facilitated potential identification of mineral emplacement targets.

Asadi (2001) used aeromagnetic data, Landsat Thematic Mapper (TM), geological and mineral occurrence data to map the gold potential at Takab area of Northwest Iran.

Kiafeng et al., (2007) in their work used Advanced Spaceborne Thermal Emission and Reflection Radiometer (ASTER) radiance data to map Lithologies related to gold deposit in the South Chocolate Mountains area, California. They compared different methods for extracting mineralogic information from ASTER data and also compared the remotely derived maps to the mapped field geology, and used the ASTER data to map minerals and lithologies related to gold exploration.

Andrada-de-Palomera (2004) used Landsat ETM+ and ASTER image to map the potential gold areas in the Deseado Massif, Southern Argentina. He extracted the mineralogical indicative features from the ASTER data and the indicative hydrothermal alteration from Landsat data and integrated these data with other geologic data such lineaments.

Kruse (1988) also used an Airborne Imaging Spectrometer data to map minerals associated with hydrothermally altered rocks in the Northern Grapevine Mountains, Nevada and California, U.S.A. Kruse (1998) continued his work on mineral exploration by illustrating the potential of hyperspectral data and how these data can be used as a tool to aid detailed geologic mapping and exploration

Sultan et al. (1986) used Landsat TM Red Green Blue (RGB) band ratios (5/7, 5/1, 5/4 * 3/4) for mapping serpentinites in the Eastern Desert of Egypt. Similar work was done by Gad and Kusky, (2006). They used Landsat ETM+ band ratio images (5/3, 5/1, 7/5) in RGB and (7/5, 5/4, 3/1) in RGB for mapping serpentinites in the Barramiya area in the Central Eastern Desert of Egypt. Amer et al., (2008) also proposed new ASTER band ratios ((2+4)/3, (5+7)/6, (7+9)/8) in RGB by analysis of the image spectra of the ophiolitic rocks at Fawakhir, Central Eastern Desert of Egypt.

Kaisser et al. (2004) used Landsat ETM+ image to map potential gold deposit in Wadi Alaqi District in Egypt. They used the band ratio technique (i.e., mineral ratio and hydrothermal ratio) to discriminate different lithology types for geological mapping.

Ferrier and Wadge (1996) used data from the Short Wave Infrared (SWIR) part of the electromagnetic spectrum to map the general location and amount of hydrous alteration minerals at a site in Southern Spain. Being able to locate these minerals, which are associated with gold mineralisation, is important for discovery of gold deposits.

Madani and Eman (2000) utilized the SWIR ASTER band ratio technique in collaboration with field verification and petrographic studies for mapping the Precambrian igneous and metamorphic rocks as well as barite mineralisation exposed at EL Hudi area in Egypt.

Bennett et al. (1994) in their exploration work utilized the TM imagery to identify mineralisation in the Santa Teresa District, Sonora, Mexico.

2.3 Spectral Signature of Minerals and Rocks

Rajesh (2004) stated that, since Hunt (1979) and co-workers, a number of papers have provided both exhaustive libraries of laboratory spectra of minerals and rocks, and accurate analysis of the absorption features of specific minerals in the visible-short wave infrared, mid- infrared and thermal infrared intervals, which result in establishing the scientific background for the interpretation of remotely-sensed spectroscopic data. Spectroscopic criteria are widely applied in hyperspectral image analysis for mineral and alteration identification and mapping. Comparing spectra of freshly cut rocks with those of exposed surfaces gives an insight into the relationship between original rock and superficial alteration products, allowing the development of reconnaissance criteria that may also be applied in other areas with similar environmental conditions.

Mineral structures are such that numerous absorption bands exist due to electronic transitions and ion vibrations (Hunt, 1977). Although minerals are of widely varying types, electronic transitions are most often created by iron, while vibrational ones are often created by water, hydroxyl ions or carbonates (Rajesh, 2004).

Vibrational transitions produce reflectance anomalies in the near infrared region of the spectrum, between 1.1 and 2.5µm, and they provide more information about the mineralogical rock composition than the spectra features observed in the visible and near infrared regions (Hunt and Ashley, 1979).

Carbonates give rise to a number of absorption features in the SWIR of which around 2.3µm is most prominent. The mid infrared region contains high reflectance anomalies for most rocks (basalt, gabbro, etc.) and minerals (clays, micas, sulphates, carbonates) at around 1.65μm and high absorption at approximately 2.2μ m (Hunt, 1979).

Rock spectra are mixtures of those for each of their constituents, proportional to their abundance. It has long been known that rocks can be distinguished from each other under ideal conditions by their spectral signatures in the thermal emission region of the spectrum (Lahren et al., 1988; Sabine et al., 1994).

2.3 Hydrothermal Alteration

Mineral deposits are commonly associated with hydrothermal alteration of the surrounding rocks, the style and extent of the alteration reflecting the type of mineral deposit (Rajesh, 2004). Laboratory studies of the near-infrared spectral properties of the rocks and minerals indicate that mineral species associated with hydrothermally altered rocks can be identified (Hunt et al., 1971; Hunt, 1979; Hunt and Ashley, 1979). The host rocks of hydrothermal mineral deposits invariably show the results of their chemical interactions with the hydrothermal fluids that caused mineral deposition (Pirajno, 1992). Such alteration commonly forms a halo around the mineralisation, providing an exploration target considerably larger than the deposit itself. The delineation and characterization of hydrothermal alteration can therefore be of great value in mineral exploration and assessment of new targets. The spatial distribution of hydrothermally altered rocks is a key to locating the main outflow zones of hydrothermal systems, which may lead to the recognition of mineral deposit (Rajesh, 2004).

According to Rajesh (2004), the colour of the rock is a good key to the identification of these minerals. When iron oxides are present the rock colour is red, brown, orange or yellow and the presence of clay minerals usually gives pale colours (yellow, violet, green, beige).

Landsat TM images are useful for hydrothermal mineral identification because of the availability of mid infrared bands in which the characteristic spectral features of most hydrothermal minerals are present. The image processing with the aim of identifying alteration minerals includes application of band combinations, band ratios, and/or Principal Component Analysis (PCA). Using Landsat TM data, an image incorporating ratios of bands 5 and 7 (TM5/7; clay mineral index), bands 3 and 1 (TM3/1; iron oxide index), and bands 5 and 4 (TM5/4; ferrous index) will highlight areas where concentrations of these minerals occur, thereby discriminating altered from unaltered ground.

Clay minerals are characteristic of hydrothermal alteration in rocks and are therefore useful indicators for mineral exploration when using Remote Sensing. According to Jian and Philippa (2009), the diagnostic spectral feature of clay minerals, which differentiates them from unaltered rocks, is that they all have strong absorption in the spectral range around 2.2μm (corresponding to TM band 7) in contrast to high reflectance in the spectral range around 1.6μm (corresponding to TM band 5).

In arid and semi-arid regions, out cropping hydrothermal alteration zones are mineralogically conspicuous enough to be detected successfully from Landsat TM data (Amos and Greenbaum, 1989; Fraser, 1991; Spatz, 1997). In tropical regions, however, high vegetation density can critically limit the successful application of Landsat TM data to the detection and mapping of hydrothermally altered rocks (Siegal and Goetz, 1977). The remote detection of iron oxide and clay zones in the presence of vegetation, however, is difficult due to similarities in the reflectance spectra of the materials. Different techniques for image processing of Landsat TM to detect and map hydrothermally altered rocks are hence aimed at separating or reducing substantially the spectral effects of vegetation from the spectral effects of the underlying substrate (Fraser and Green, 1987). Spectral unmixing (Smith et al., 1985) is one such technique and endeavours at searching the abundances or fractions of pure spectral components, so called end members, which best explain the observed mixed pixel spectra. PCA of images has been shown to be a successful tool to minimize the vegetation effect in the resulting images (Kaufman, 1988; Loughlin, 1991; Fraser, 1991; Bennett et al., 1993; Ruiz -Armenta and Prol- Ledesma, 1998; Tangestani and Moore, 2001).

2.4 Lineament

According to O'Leary et al. (1976), lineaments are linear features shown on Remote Sensing Imagery. Regional study of linear features such as fault, joints, dikes, crustal fracturing, and lithological contacts using aerial photographs and particularly satellite image, has made important advances in geological research during the last few decades (Rowan and Lathram, 1980). Recognition of lineament has been used for investigating active fault patterns in areas of difficult accessibility (Tibaldi and Ferrari, 1991), mineral deposit exploration (Rowan and Lathram, 1980), and in the study of the structural or tectonic history of a region.

Sijmons (1987) distinguished between two categories of computerised lineament processing. The first involves mainly enhancement of linear features using standard image processing methods such as edge detection directional filters for later visual interpretation while the second category involves automatic computer processing of the original digital data for the production of lineament map.

Many studies have emphasized the importance of lineament interpretations and digital lineament analysis in localizing the major mineral deposits and notes that there is a strong correlation between mineral deposits and lineaments (Kutina 1969; Katz 1982; Liu et al., 2000; Rein and Kaufmann, 2003).

Lineament map can be produced from Remote Sensing image by visual interpretation and manual digitising or by automatic extraction. Different authors such as Budkewitsch et al., (1994); Karniel et al., (1996); Lepage et al., (2000); Madina, (2001); Vassilas et al., (2002) have automatically extracted lineaments by using different methods which include edge detection, thresholding and image classification.

Rokos et al., (2000) and Suzen and Toprak (1998) applied Laplacian high frequency spatial filters and directional filters. Asadi (2000) also used PC1 from a principal component analysis as this is the principal component that explains most of the topographic information to enhance lineaments before manual digitising on the computer screen. Rein and Kaupfmann (2003) used TM RGB colour composites such as 721, 742 and 721 to enhanced lineaments for visual interpretation.

2.5 Band Ratio Technique

The band ratioing method is one of the simplest methods for multispectral image enhancement technique (Jain, 1989). A band ratio is created by dividing spectral values of one band by spectral values of another band from a multispectral image. It is usually applied to enhance the spectral differences between surface covers that are difficult to detect or separate in raw images. It suppresses the effect of variable illumination resulting from topographic variations (Mather, 1987), and eliminates slope shadows, seasonal changes, and either differences in sunlight angle or intensity

(Apan et al., 2002). The differences in pixel brightness of the ratio image are caused by only differences in reflectance without effects of topography and hence the classification of ratio values will produce classes of uniform spectral properties, regardless of topography. Crippen's four-component technique uses three band-ratio images (one each for the red, green, and blue output channels) for the chromatic components of the image (Crippen et al., 1990). The three ratios, 3/1, 5/7, and 5/4 of the four-component technique are useful for their sensitivity to lithologic variables, and for their lack of statistical redundancy (Crippen, 1989; Crippen et al., 1988).

2.6 Landsat Enhanced Thematic Mapper

Landsat Enhanced Thematic Mapper (ETM+) has 9 spectral bands. These bands include three visible bands (1-3) between 0.4 and 0.7µm and one near infrared (NIR) band (4) between 0.76-0.90µm and two infrared (IR) bands (5 and 7) between 1.55 and 2.35µm, and one panchromatic band 8 between 0.52-9.0µm; in addition, two thermal infrared bands (61 and 62) between 10.40 and 12.5µm. Landsat ETM+ spectral bands have a spatial resolution of 30 meters for bands 1 to 5 and band 7. The resolution for band 6 (thermal infrared) is 60 meters and resolution for band 8 (panchromatic) is 15 meters.

2.7 Mineral Potential Mapping

Nykänen (2011) stated that prospectivity mapping is used to define areas favourable for mineral exploration and can be applied in various scales from global to local scale exploration targeting. GIS provide a flexible and powerful platform to apply spatial data analysis techniques as a tool for prospectivity mapping by integrating Remote Sensing data, geochemical, geophysical and geological data. According to Nykänen, (2011) there are two methods of spatial data analysis used for prospectivity mapping and these are the Data-driven Approach and the Knowledge-driven Approach. See Table 2.1

Table 2.1: Comparison of the Data-driven Approach and Knowledge-driven Approach.

Empirical (data-driven) Approach	**Conceptual (Knowledge-driven) Approach**
Suitable for mature 'brown fields' exploration terrains with abundant data available	Suitable for 'green fields' exploration terrains with limited number of deposits available for statistical assessment
Known mineral occurrences as 'training points' are used for examining spatial relationships between known occurrences and particular geological, geochemical and geophysical key features	Re-formulation of knowledge about deposit formation into mappable criteria (i.e, threshold values in geochemistry and geophysics etc., certain structures or formations in the geological maps.)
Identified relationships are quantified and integrated into a single prospectivity map	Areas that fulfil the majority of these criteria are highlighted as being the most prospective
•Neural networks (RBFLN, PNN etc.) •Weights of evidence, logistic regression	•Boolean logic •Index overlay (binary or multi-class maps) •Evidential belief function

Source: Nykänen, (2011)

Traditionally, prospectivity mapping was based on expert opinions on potential areas for a certain deposit type but digital maps now allow quantitative analysis of data and numerical modelling for prospectivity mapping (Nykänen, 2011).

Mineral potential mapping with digital data sets was practised in research organisations prior to the arrival of commercial GIS (Bonham-Carter, 1997).

The Data-driven Approach requires that quite extensive exploration has taken place in the region of interest, so that adequate samples of mineral occurrences of the right type are known. The spatial association between the known occurrences and the predictive data sets is used to determine weights, and the weights are then applied to predict areas with similar characteristics to the known occurrences.

The Knowledge-driven Approach can be quite simple, using subjective weights and an additive model, or can employ more sophisticated knowledge-representation tools such as fuzzy membership functions.

2.8 Weights of Evidence (WofE) Method

Weights-of-evidence is a Data-driven technique used to combine datasets. It uses a log-linear of the Bayesian probability model to estimate the relative importance of evidence by statistical means and requires training sites. It has been applied to combine evidences in various fields of disciplines such as in quantitative medical diagnosis, ecology and geology (Bonham-Carter, 1994).

Washington Franca-Rocha et al. (2003) stated that the pair of weights (W+ and W-), is determined from the degree of overlap between the training points and the evidential themes. If there is no spatial association between the training points and the evidential theme, then W+ = W- = 0 while a positive weight(W+) value indicates a positive association between training points and the evidential theme. This means that, more of the training points occur on the evidential theme class than would be expected if the number of training points occurring in the evidential theme class could be due to chance. On the contrary, a negative association implies the occurrence of fewer training points on that evidential theme class than would be expected due to chance.

The contrast value C, where C = W+ - W- , is a summary value that reflects the degree of spatial association between the evidence theme and the mineral prospects. The larger the C value, the greater is the spatial association. A study of weights and contrast values can facilitate the process of identifying breaks between background and anomalous values in geochemical data, or in identifying critical distances on evidential themes related to proximity to spatial objects (Bonham-Carter, 1994).

CHAPTER THREE

3.0 MATERIALS AND METHOD

3.1 Study Area

The study area is shown in figure 3.1.

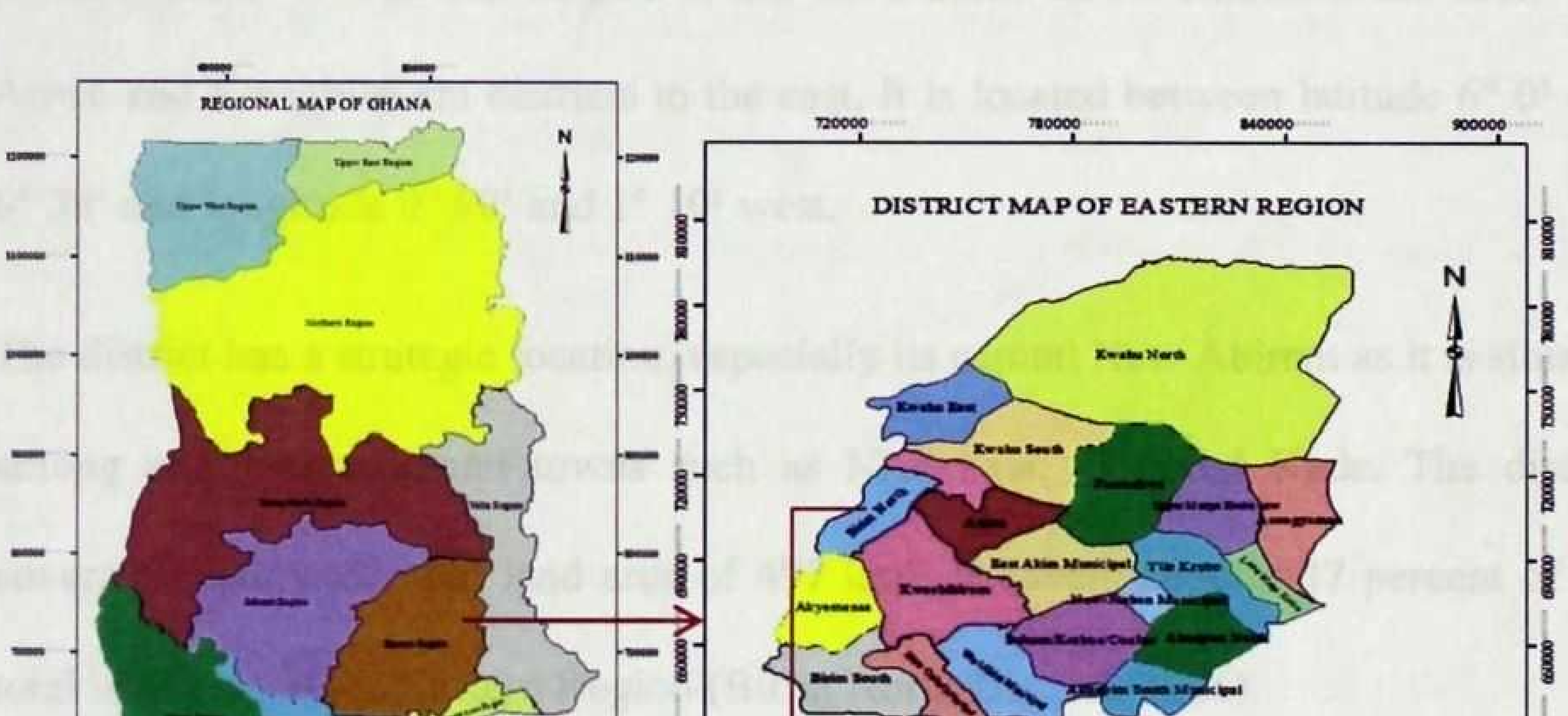

Figure 3.1: Map of the study area [(*A*): Regional map of Ghana (*B*): District map of Eastern Region of Ghana and (*C*): Landsat ETM+ image of the study area as displayed in RGB: 432].

3.1.1 Location and Size of the District

The Birim North District was formed from former Birim District Council in 1987 as part of the Government's decentralisation programme to promote effective decentralised governance and speed up the development of the area. It is bordered by Kwahu West to the north, the Asante Akyem South, Amansie East and Adansi South districts, all in the Ashanti Region to the west, Birim South district to the south and Atiwa and Kwaebibirem districts to the east. It is located between latitude 6° 0' and 6° 30' and longitude 0° 90' and 1° 10' west.

The district has a strategic location, especially its capital New Abirem as it is situated among major commercial towns such as Nkawkaw, Oda and Kade. The district covers an estimated total land area of 497 km^2. It covers about 6.47 percent of the total land area of the Eastern Region (Birim North District, 2006).

3.1.2 Relief and Drainage

The district is mostly undulating and mountainous in nature. The hilly areas of the district rise to over 61 metres above sea level (Birim North District, 2006). The district is drained mainly by two great and historical rivers, the Pra and its tributary the Birim (Birim North District, 2006).

3.1.4 Geology and Soil Types

Greater part of the district is underlain with granite and both upper and lower Birimian rock formation of phylite, schist, greywacke and metavolcanic and quartzes. These rocks have high potential for ground water extraction. The district lies almost wholly in the main mineral deposit area of the region accounting for the large mineral prospecting and exploration by a number of firms and small scale mining operation in gold and diamond (Birim North District, 2006).

The soils of the district can be classified into five broad categories. These are:

1. The Swedru-Nsaba/Ofin Compound Association is the predominant soil formation found in the district. These soils were developed over granite and can be found around Pankese in the northern part of the district. It is also predominant around Nkwateng, stretching south of Otwereso and westward to Abenase. This compound association consists of two simple associations, Swedru-Nsaba Association and Nta-Ofin Association, the latter being developed from the transported products of the erosion of the former Swedru series. They occur on nearly flat summits and gently to moderately steep upper slopes. The Swedru-Nsaba series are high in magnesia and potash and are very good soils for tree and arable crops, and are particularly excellent for cocoa. Ofin soils are unsuitable for tree crops and mostly used for growing dry season vegetables, sweet potatoes, sugarcane and rice.
2. The soil in the Atewa-Atukrom-Asikuma-Ansum compound series are found around the Amuana Praso area. This soil type is restricted to a smaller part of the district. This type of soil consist of dark brown slightly humus silty clay loam top soils overlying reddish brown to red silky clay loam subsoils. Generally, these two soil series are infertile because of strong acidity and low base status. The soils are recommended for coffee, oil palm, other tree crops and forestry.
3. Juaso-Manso-Adubea Association can be found around Noyem stretching south to Praso kuma and to the east as far as Atobiaso. This soil type is dark brown and shallow. This type of soil supports the production of oil palm.
4. The Bekwai-Oda Association can be found around New Abirem stretching to Ntronang. The Bekwai series are well drained and are suitable for the

production of a wide variety of tree and arable crops such as cocoa, coffee, citrus, oil palm, avocado pear, mangoes, yams, maize, cassava and plantain. The Oda series occupy also flat, fairly extensive lands adjacent to rivers and streams and are well suited for mechanized irrigated rice farming.

5. The Birim-Chichiwere Association which is restricted to the south-eastern part of the district around Edubia was developed over the River Birim deposits. Birim series are moderately well drained, deep and easy to work with machines. They occur on almost flat lands where susceptibility to erosion is virtually nil or very slight. They are suitable for a wide range of tree and arable crops. Chichiwere series on the other hand are generally considered bad for tree crops (Birim North District, 2006).

3.2 Criteria for the selection of Study Area

Data were readily available for the research work. The exploration of gold deposit by using Remote Sensing Imagery and GIS will help discover all the possible gold deposits in the study area for future exploration works.

3.1.3 Climate and Vegetation

The district lies within the wet semi-equatorial climatic zone that experiences substantial amounts of precipitation. It experiences a double maxima rainfall pattern. The first rainfall season starts from late March to early July and the second season is from mid-August to late October. The amount of rainfall received in the district is between 150 cm and 200 cm reaching its maximum during the two peak periods of May-June and September - October yearly (Birim North District, 2006).

Temperatures range between an average minimum of 25.2 degrees Celsius and a maximum of 27.9 degrees Celsius. The district has a relative humidity of about 55-59 percent throughout the year. The district lies within the Semi-deciduous forest belt of Ghana comprising tall trees with evergreen undergrowth. The forest contains large species of economic trees (Birim North District, 2006).

3.3 Materials

The materials used in this research work are listed below:

1. Gold occurrence points to be used as training sample.
2. Geologic map of Birim North District (Ghana Geological Survey, 2005).
3. Remote Sensing Image (ETM+) of the study area from Landsat (The Landsat ETM+ image which was acquired on the 15th January, 2002 from Landsat.com. The image has WRS Path of 194 and WRS Row of 056). The resolution is 30 meters.
4. Geophysical data of Birim North District (2010).
5. Geochemical data of Birim North District (2010).
6. ERDAS Imagine 2010, Version 10.1 produced by The Earth to Business Company.
7. ArcGIS 10.1 and ArcView 3.3 produced by ESRI.

3.4 Method

The flowchart of the method used in this research work is illustrated in Figure 3.2. Georeferencing was rather performed on the geologic map of the study area because of difference in coordinate system between the geologic map and the image and this form the vector layer. Pre-image processes such as stacking and subseting were performed on the ETM+ image to obtain the image of the study area. Some image enhancement techniques such as band combination, band ratio, and principal component analysis were also performed on the image of the study area for the extraction of hydrothermal alteration and this form the raster layer. The band ratio was applied on the ETM+ image in order to enhance the spectral differences that are difficult to detect in a raw image. It also eliminates the difference in sunlight angle or intensity. The principal component analysis was performed on the image by using the first three components and the principal component analysis was a good way to find the different rock types as the analysis was able to separate the different rock types. However, some local information was needed in order to tell what each component is related to since the components do not carry out material information directly. It was only useful in identifying the various rock types within the study area rather than identifying altered rocks associated with gold mineralization.

An edge enhancement filter specifically low pass kernel size filter was applied on the geophysical aeromagnetic image to highlight the lineament for on screen digitizing. The aeromagnetic image was used because it maps the unseen or below geology as against the satellite image which only maps the surface ground cover. The point soil geochemical data of the study area was first of all converted into a continuous surface representation by using the inverse weighting interpolation in ArcGIS 2010. Then a principal component analysis in ArcGIS 2010 was applied on the surface representation of the geochemical data by using the first three components to reduce the dimensionality of the data. The first three components were used because these components account for much of data variance as possible.

The vector layer, the raster layer, the geochemical data, the geophysical data and the gold occurrence points of which some were used as training sample and the rest for validation were integrate in GIS environment to form the GIS database. By using the

ArcView weight of evidence, the training samples were used to calculate the weight for each evidential theme. Then the generalization, grouping class of the evidential themes together and identifying break or cut-off in the continuous variable were performed in order to help maximize the spatial association and this led to better understanding of the data. Finally, the weighted evidential themes were combined to produce the gold potential map of Birim North District. The posterior probability or the conditional probabilities associated with the potential map is the probability of occurrence of mineral deposit provided the conditions of the predictive evidence exist in the study area (Hongmei et al., 2002). The posterior probability is obtained by (1) calculating the prior probability of the gold deposit occurring in the study and the prior probability is obtained by dividing the total number of training samples or points by the total study area. (2) The weights are then calculated by using the training samples and the evidential themes. (3) The weighted evidential themes or maps were combined in order to estimate the posterior probabilities associated with the gold potential maps.

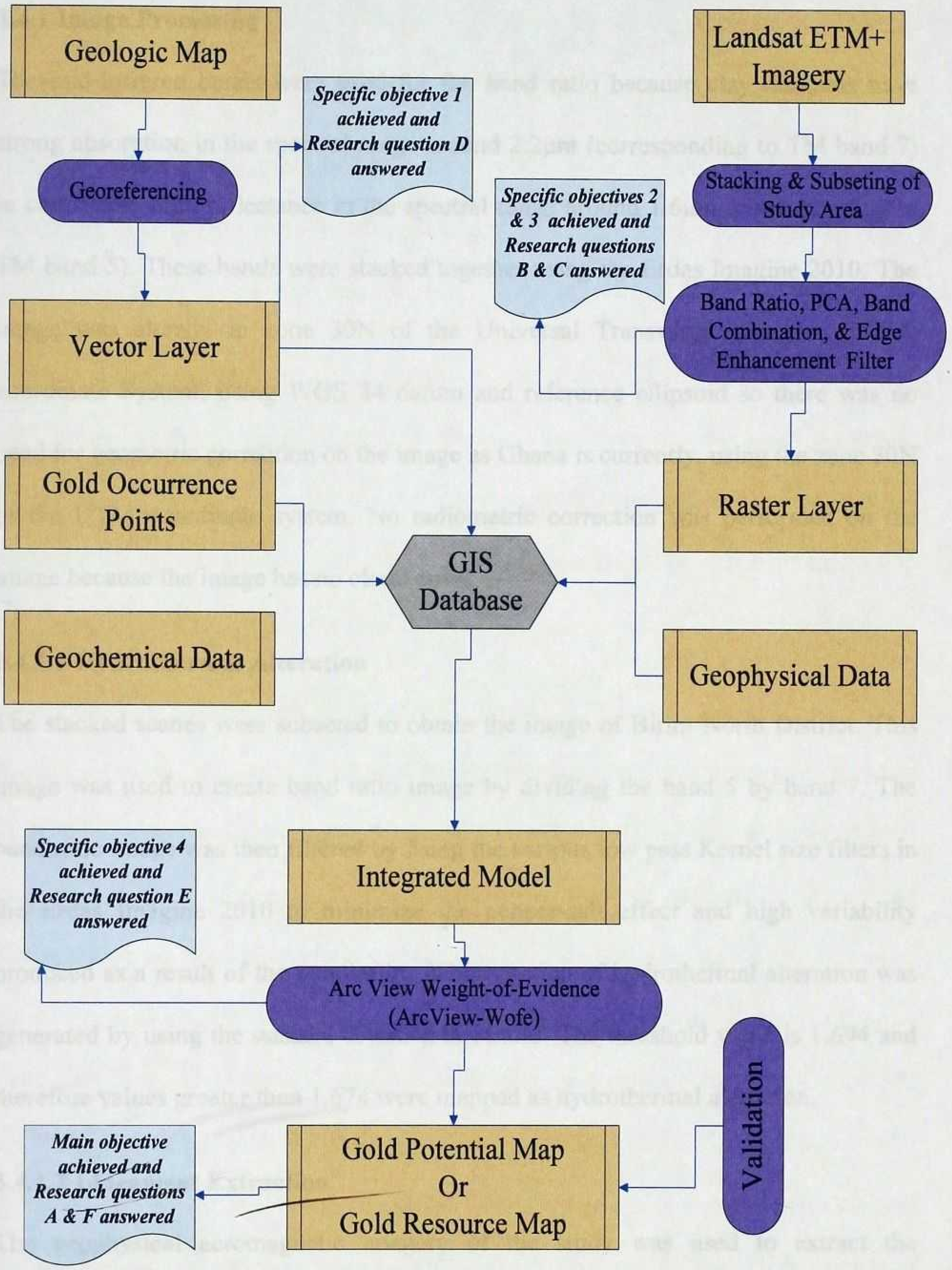

Figure 3.2: The flowchart of the methodology

3.4.1 Image Processing

The mid-infrared bands were used for the band ratio because clay minerals have strong absorption in the spectral range around 2.2µm (corresponding to TM band 7) in contrast to high reflectance in the spectral range around 1.6µm (corresponding to TM band 5). These bands were stacked together using the Erdas Imagine 2010. The image was already in zone 30N of the Universal Transverse Mercator (UTM) coordinate System, using WGS 84 datum and reference ellipsoid so there was no need for geometric correction on the image as Ghana is currently, using the zone 30N of the UTM coordinate system. No radiometric correction was performed on the image because the image has no cloud cover.

3.4.1.1 Hydrothermal Alteration

The stacked scenes were subseted to obtain the image of Birim North District. This image was used to create band ratio image by dividing the band 5 by band 7. The band ratio image was then filtered by using the various low pass Kernel size filters in the Erdas Imagine 2010 to minimize the pepper-salt effect and high variability produced as a result of the band ratio. A binary map of hydrothermal alteration was generated by using the standard deviation threshold. The threshold value is 1.694 and therefore values greater than 1.674 were mapped as hydrothermal alteration.

3.4.1.2 Lineament Extraction

The geophysical aeromagnetic imagery of the study was used to extract the lineament in the study area. The aeromagnetic imagery was used because it maps the unseen or below lithology or geology as against the satellite imagery which only maps the superficial ground-cover. An edge detection directional filter was applied on the imagery in ERDAS Imagine 2010 to highlight the lineament. The enhanced imagery was later imported in ArcMap 2010 for on screen digitizing to produce the lineament map of Birim North District.

3.4.2 Processing of Geochemical Data

Bonham-Carter (1991) stated that geochemical data plays a significant role in many spatial databases for exploration purposes.

The point soil geochemical data of the study area was first of all converted to a continuous surface representation by using the inverse distance weighting interpolation method in ArcGIS 2010 and the result. A principal component analysis in ArcGIS 2010 was applied on the surface representation of the geochemical data to reduce the dimensionality of the data.

3.4.3 Data Integration with Weights of Evidence

According to Kemp et al.(1999), GIS-based mineral potential mapping process can be broken down into four main steps and these are: (1) building a spatial digital database (2) extracting predictive evidence for a mineral deposit (3) calculating weights for each predictive map (evidential theme) and (4) combining the evidential theme to predict the mineral deposit. The weight of evidence was adapted in the late 1980s for mineral potential mapping with GIS and when using the weight of evidence for mineral potential mapping, the evidence consists of a set of exploration datasets. The weight of evidence was used because it provides a quantitative method for integrating multiple sources of evidences. It also avoids subjective choice of evidences and subjective estimation of weight for evidences as compared with other methods such fuzzy logic method.

The hypothesis is ' this location is favourable for occurrence of deposit' and the hypothesis is then repeatedly evaluated for all possible locations on the exploration dataset by using the calculated weight, thereby producing a mineral potential map from several exploration datasets or map layers when combined.

After building the spatial digital database by using the ArcGIS and extracting the predictive evidence for the gold deposit such as the lineament, hydrothermal alteration, geochemical and geophysical anomalies, a total 250 gold occurring points were used. While 180 were used as training points, 70 were used for the validation. The training points were used to calculate the weight for each exploration dataset by using the ArcView weight of evidence.

Then the generalization, grouping class of evidential theme together and identifying breaks or cut-off in the continuous variable was performed to help maximize the spatial associations which led to a better understanding of the data.

Finally the weighted evidential maps were combined to produce the gold potential map of Birim North District. The posterior probability or the conditional probabilities associated with the potential map is the probability of occurrence of mineral deposit provided the conditions of the predictive evidence exist in the study area (Hongmei et al., 2002).

CHAPTER FOUR

4.0 RESULTS AND DISCUSSION

4.1 Results

4.1.1 Result of the Band Ratio

The Figure 4.1 illustrates the result obtained when band 5 of the landsat ETM+ image is divided by band 7 of the same Landsat ETM+ image.

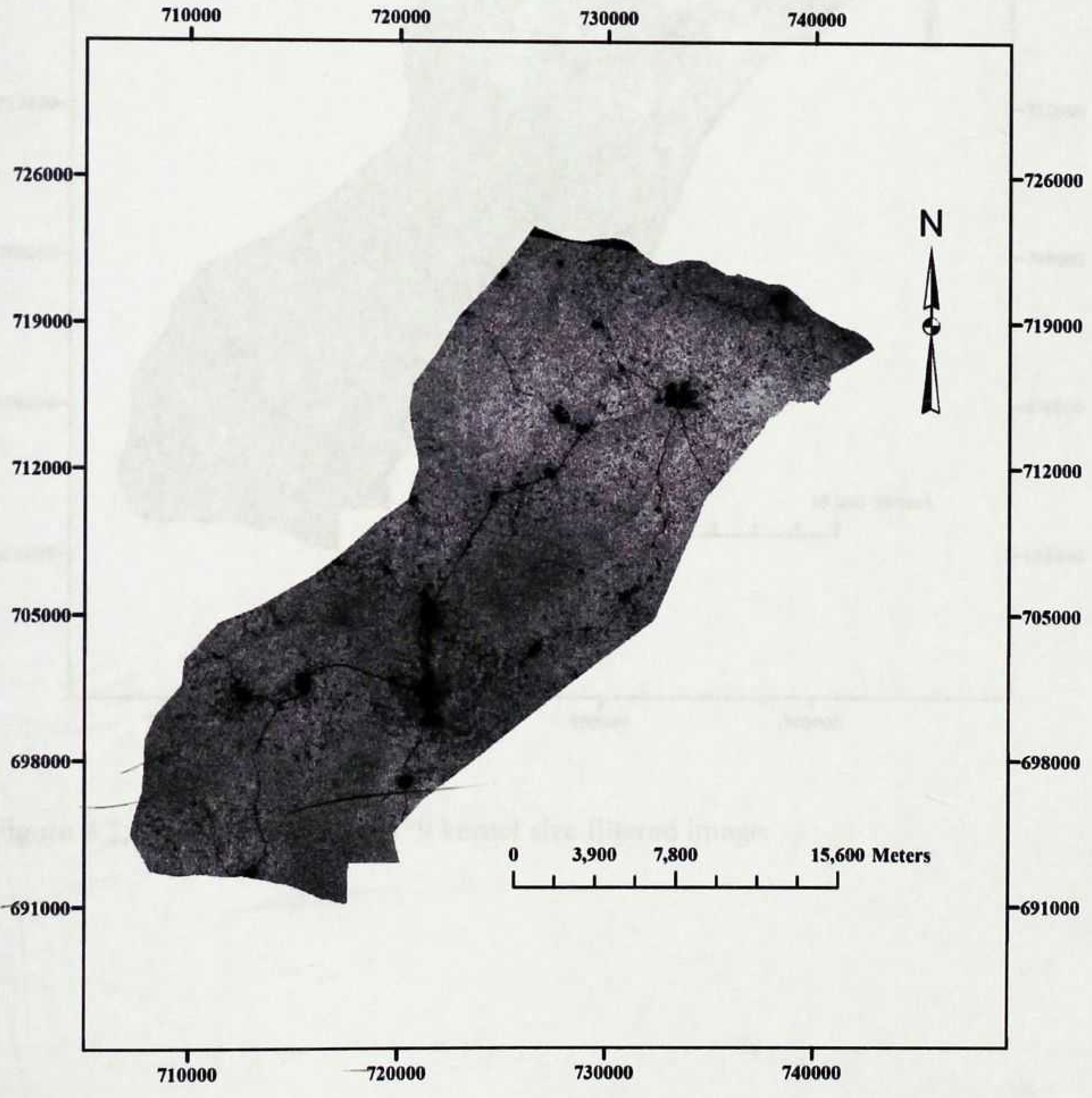

Figure 4.1: The image of Band 5 divided by Band 7.

4.1.2 Result of Low Pass 9*9 Kernel Size Filter Application

The result display in Figure 4.2 was obtained after the low pass 9*9 kernel size filter was applied on the band ratio image.

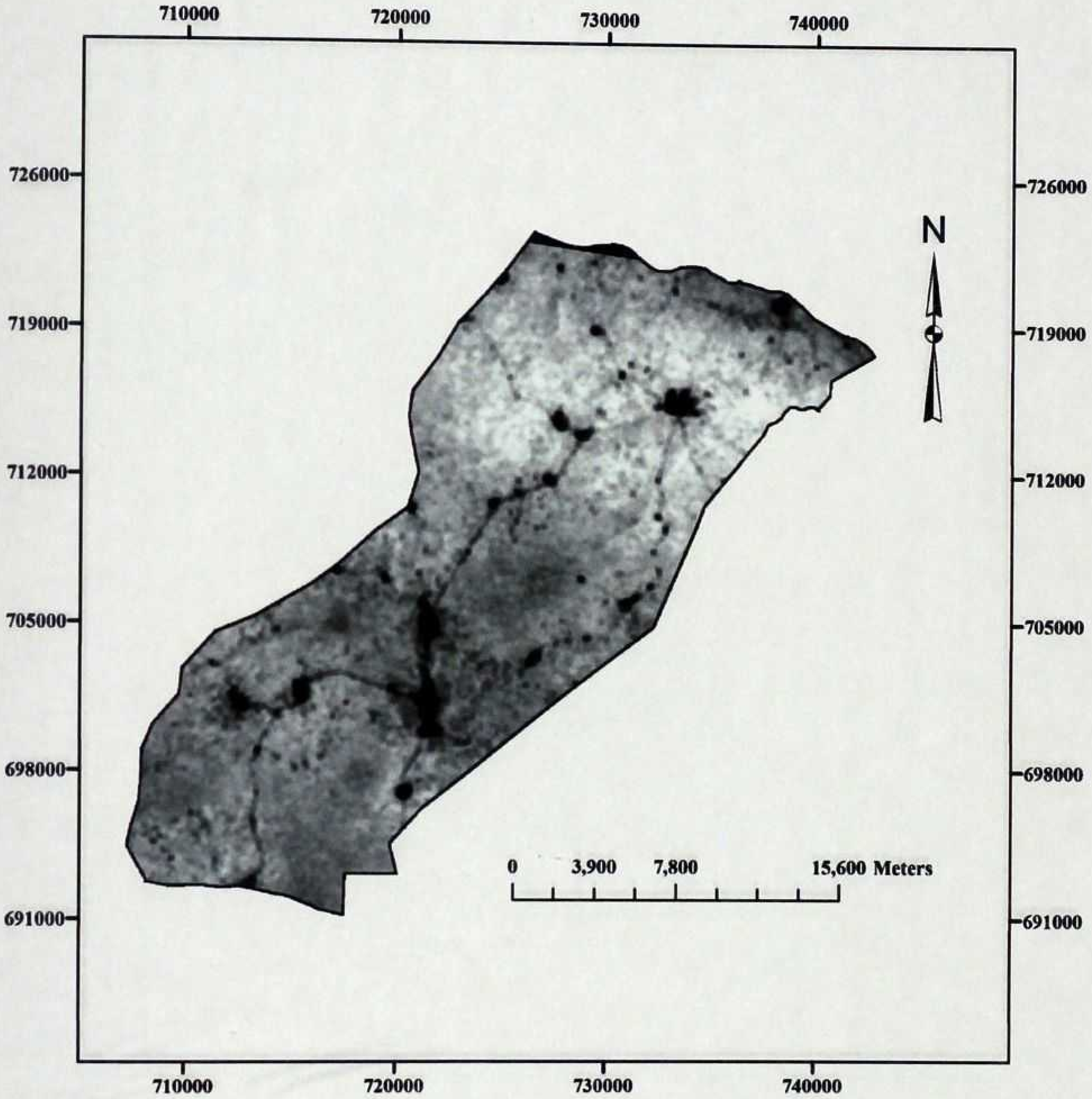

Figure 4.2: Result of low pass 9*9 kernel size filtered image.

4.1.3 Result of Low Pass 7*7 Kernel Size Filter Application

The result display in Figure 4.3 was obtained after the low pass 7*7 kernel size filter was applied on the band ratio image.

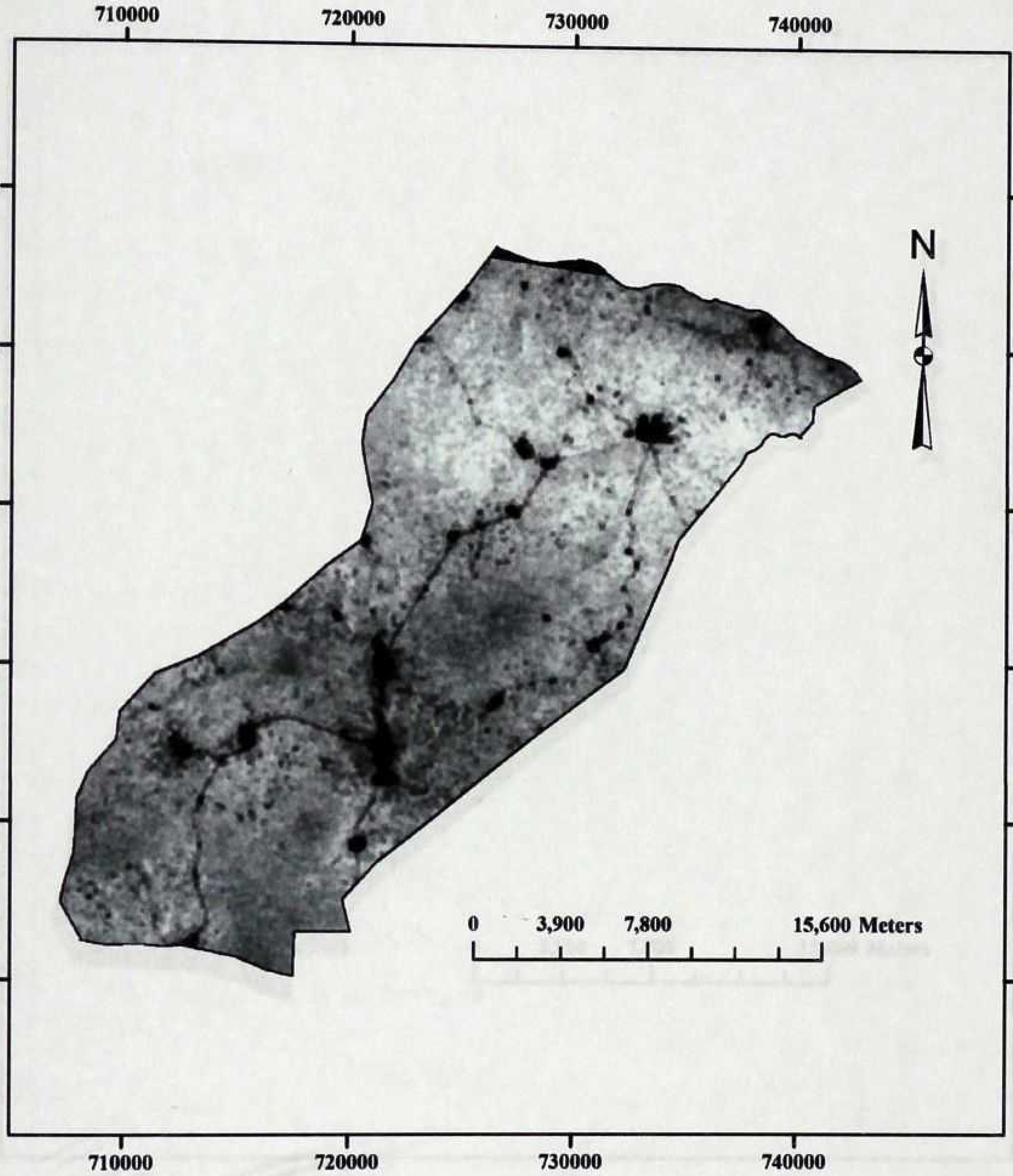

Figure 4.3: Result of low pass 7*7 kernel filtered image.

4.1.4 Result of Low Pass 5*5 Kernel Size Filter Application

The result display in Figure 4.4 was obtained after the low pass 5*5 kernel size filter was applied on the band ratio image.

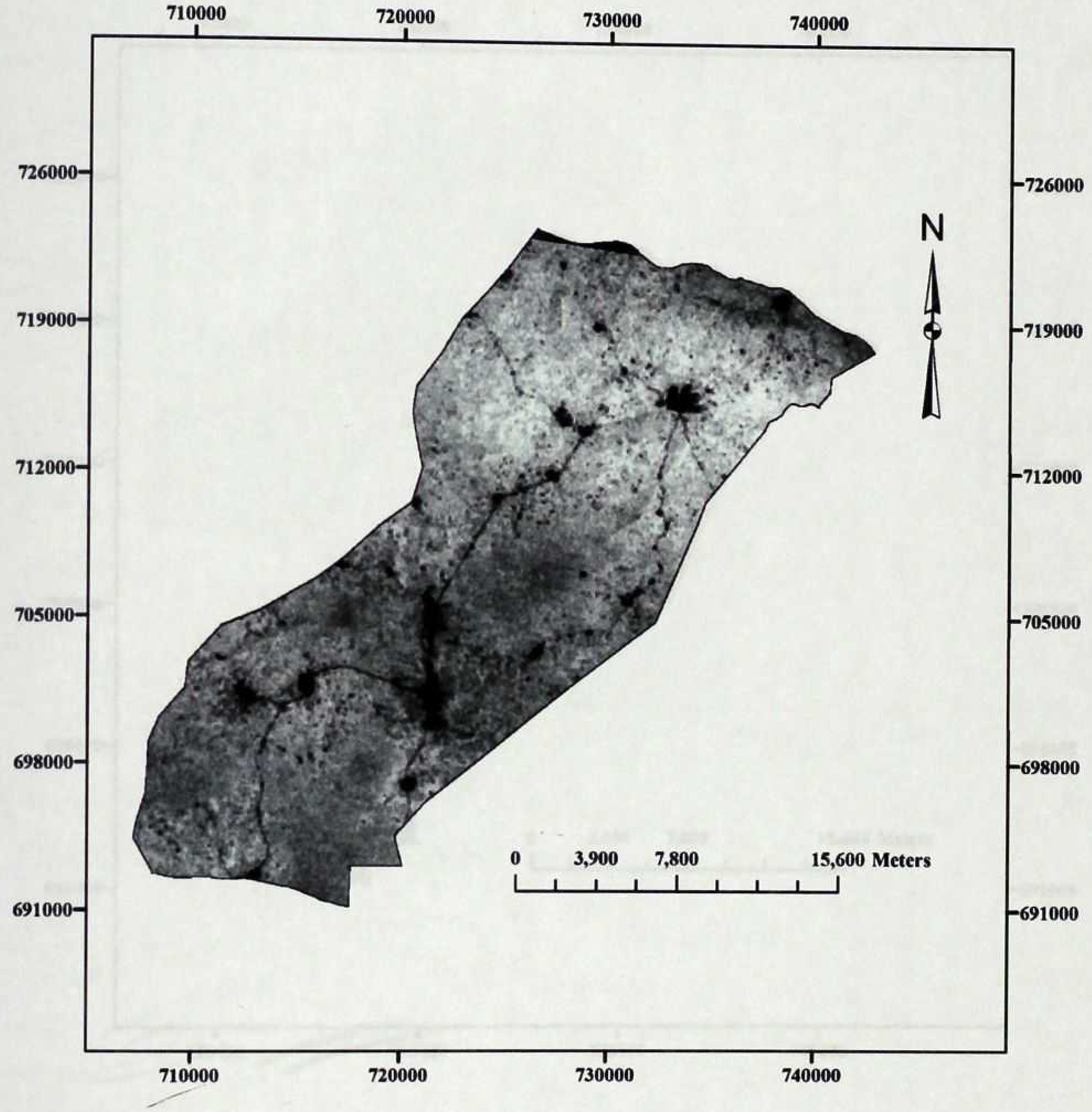

Figure 4.4: Result of the low pass 5*5 kernel size filtered image.

4.1.5 Result of Low Pass 3*3 Kernel Size Filter Application

The result display in Figure 4.5 was obtained after the low pass 3*3 kernel size filter was applied on the band ratio image.

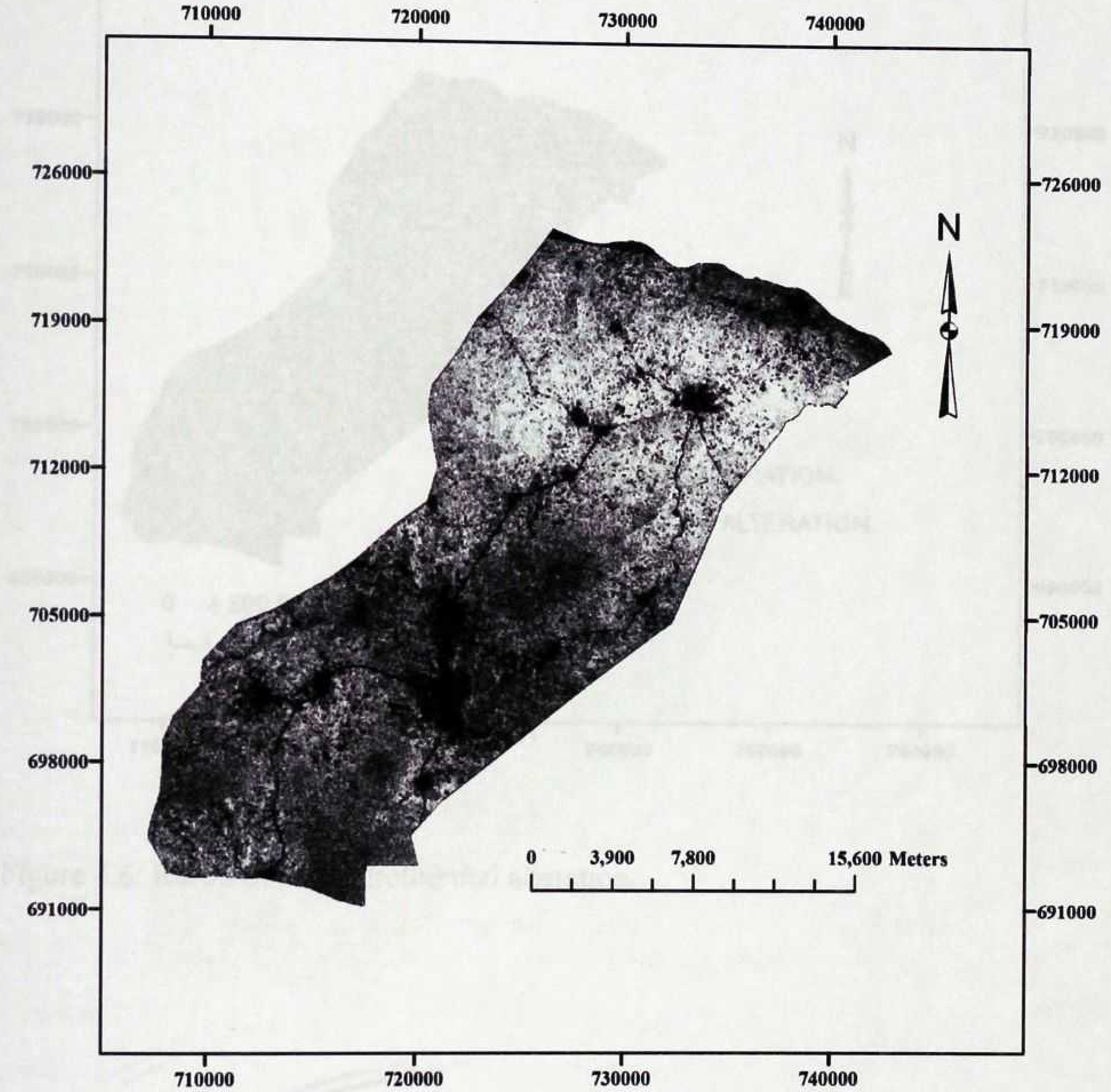

Figure 4.5: Result of the low pass 3*3 kernel size filtered image.

4.1.6 Result of Hydrothermal Alteration

The hydrothermal alteration is shown in Figure 4.6.

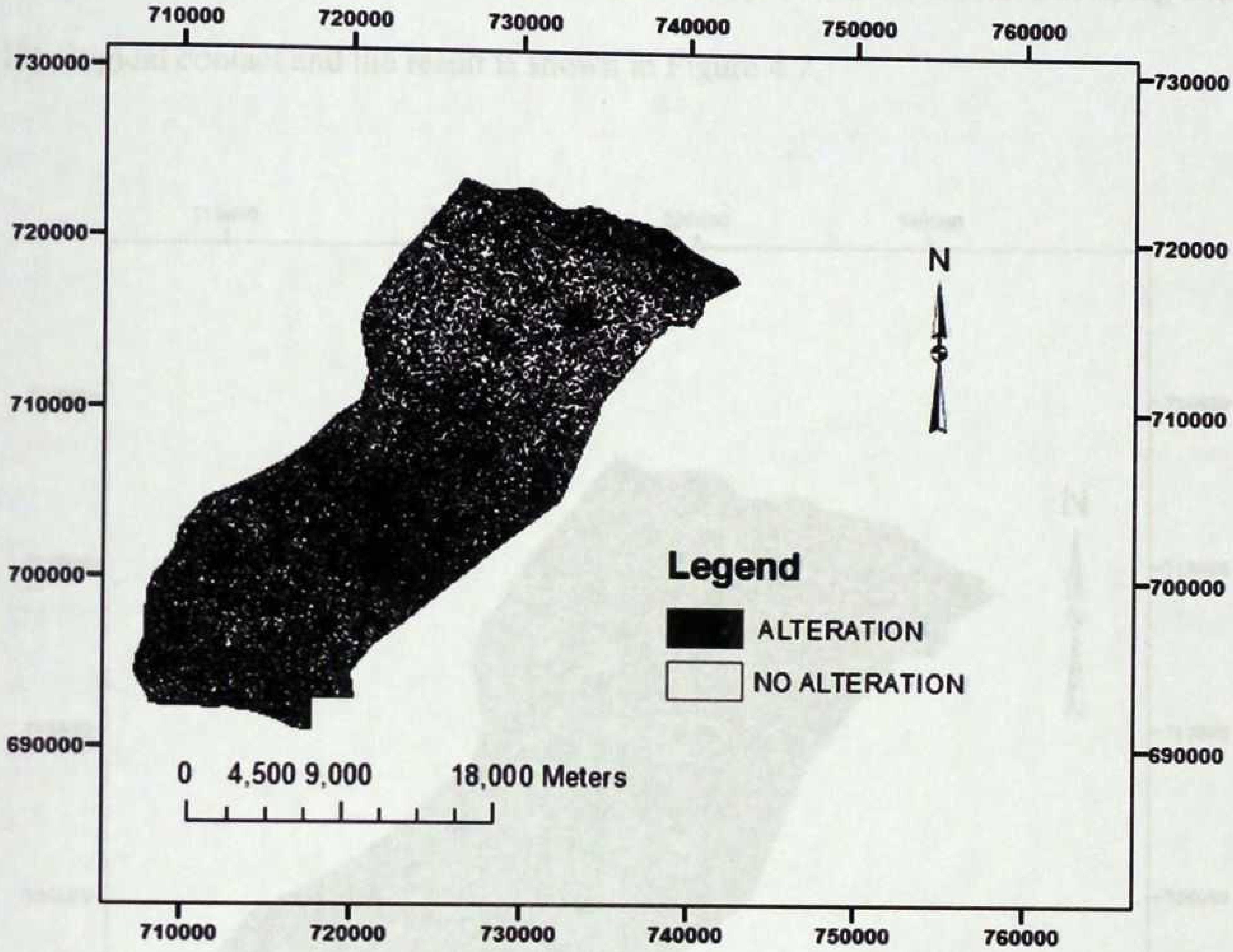

Figure 4.6: Result of the hydrothermal alteration.

4.1.7 Result of Edge Detection Directional Filter Enhancement

An edge detection dirctional filter was applied on the aeromagnetic imagery for the enhacement of the linear features such as the fault, joints, dike, crustal fracturing and lithological contact and the result is shown in Figure 4.7.

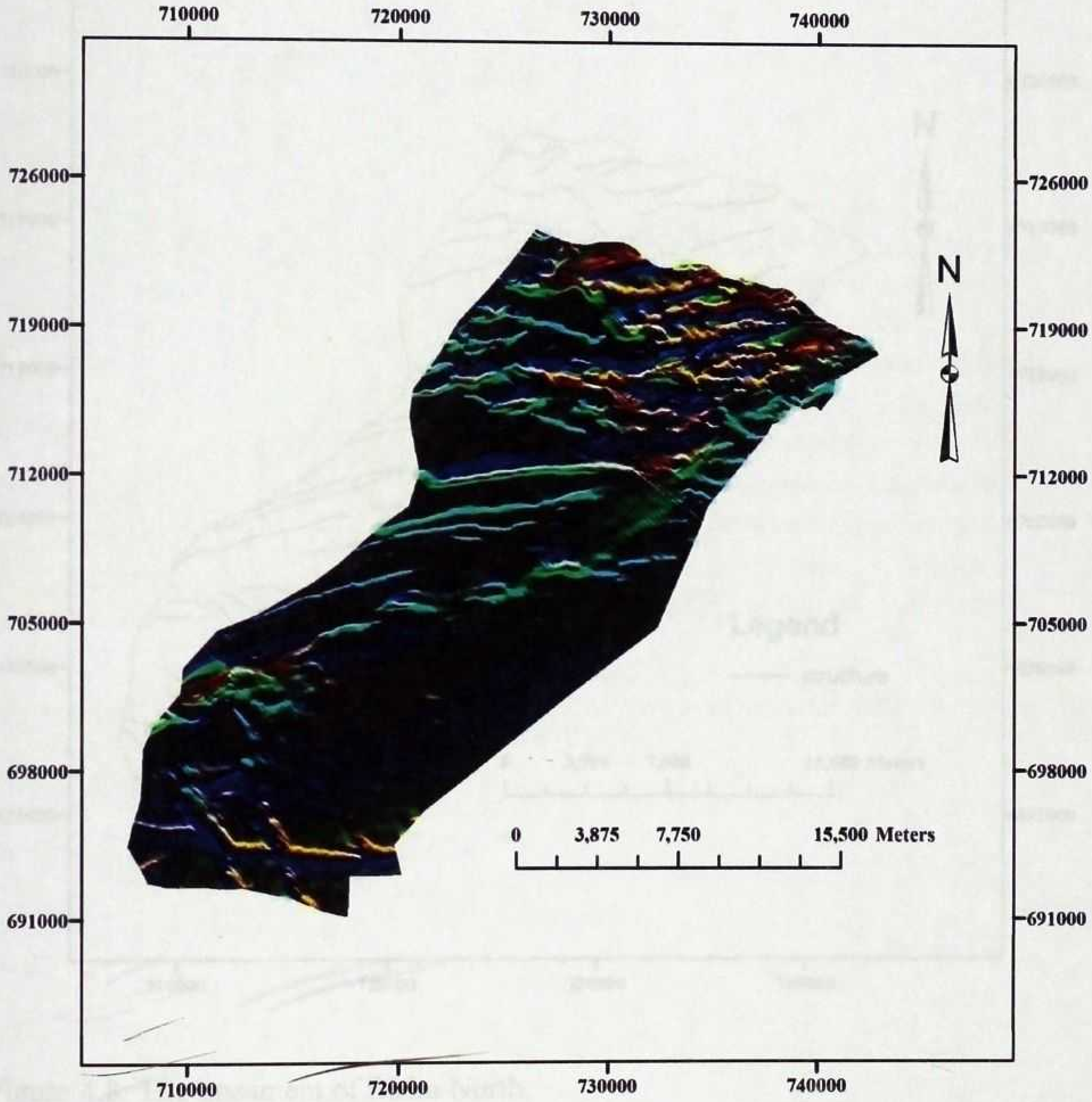

Figure 4.7: Result of the aeromagnetic image after applying the edge detection directional filter.

4.1.8 Result of Lineament Extracted from Aeromagnetic Image

Figure 4.8 below shows the result obtained after extracting lineament from the enhanced aeromagnetic image.

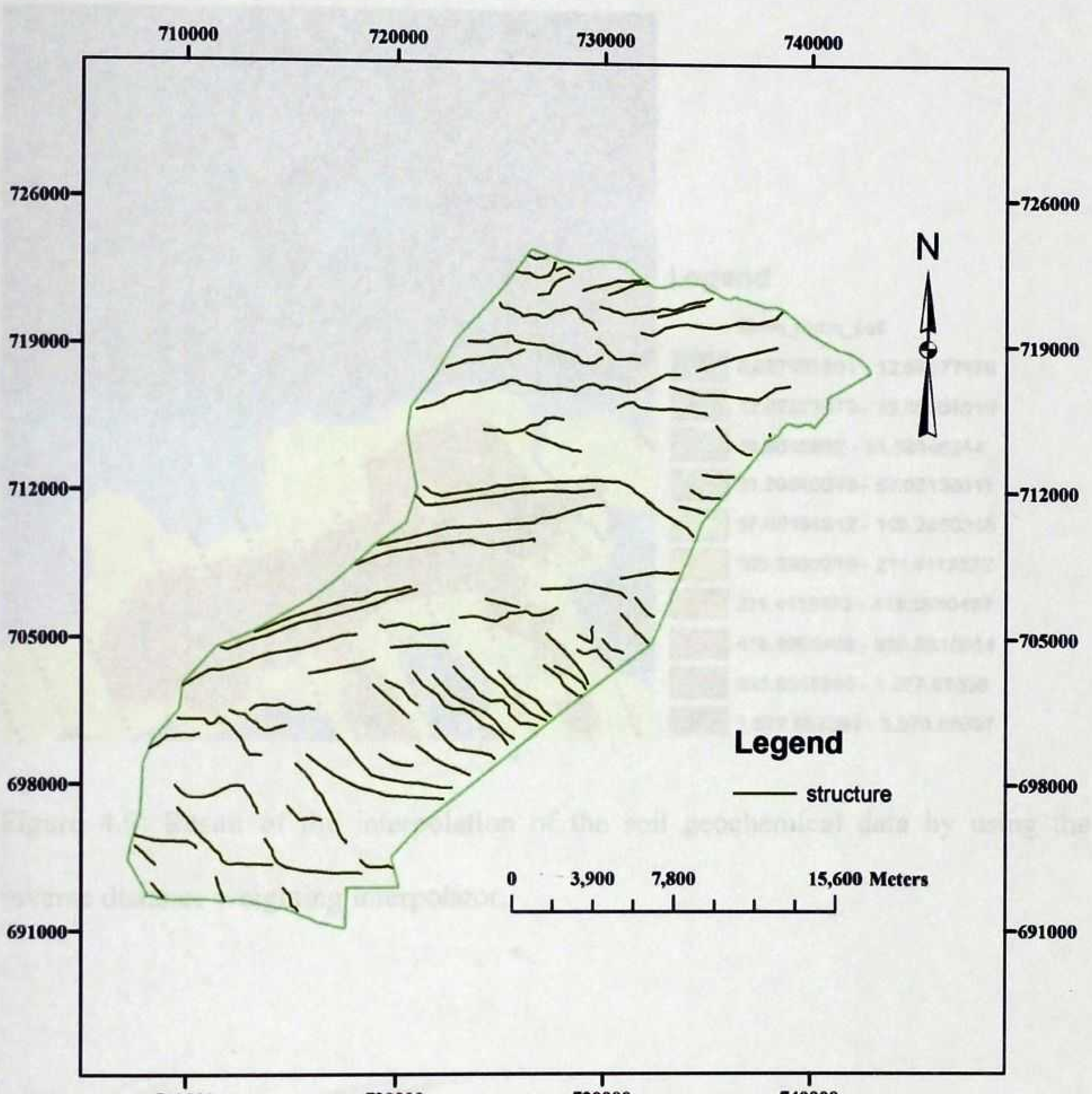

Figure 4.8: The lineament of Birim North.

4.1.9 Result of Inverse Distance Weighting Interpolation of Soil Geochemistry

The result of the interpolation of the soil geochemical data by using the inverse distance weighting interpolation is illustrated in Figure 4.9.

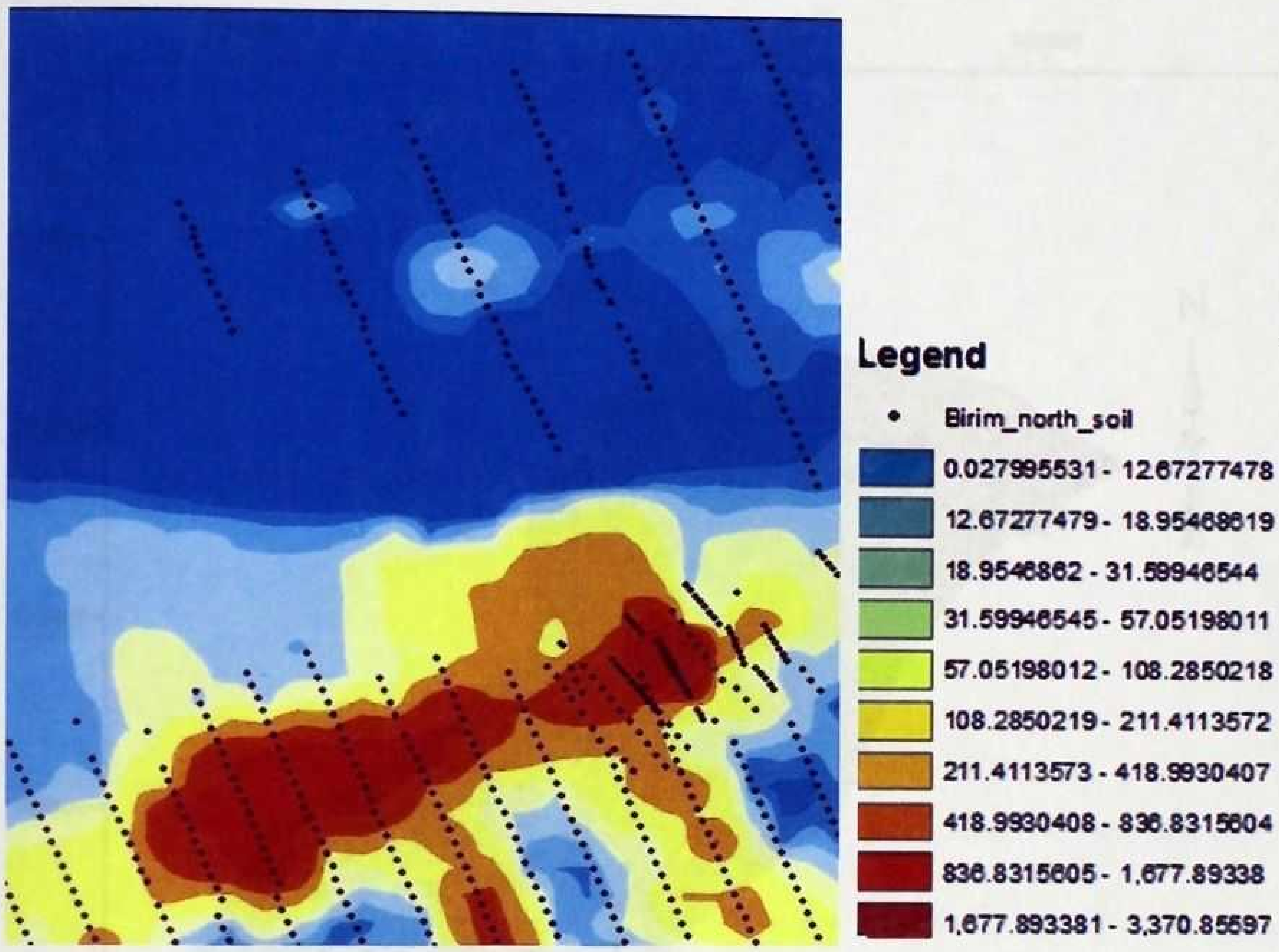

Figure 4.9: Result of the interpolation of the soil geochemical data by using the inverse distance weighting interpolator.

4.1.10 Result of Principal Component Analysis

PC1, PC2 and PC3 were the components used to compose a RGB image as shown in Figure 4.10.

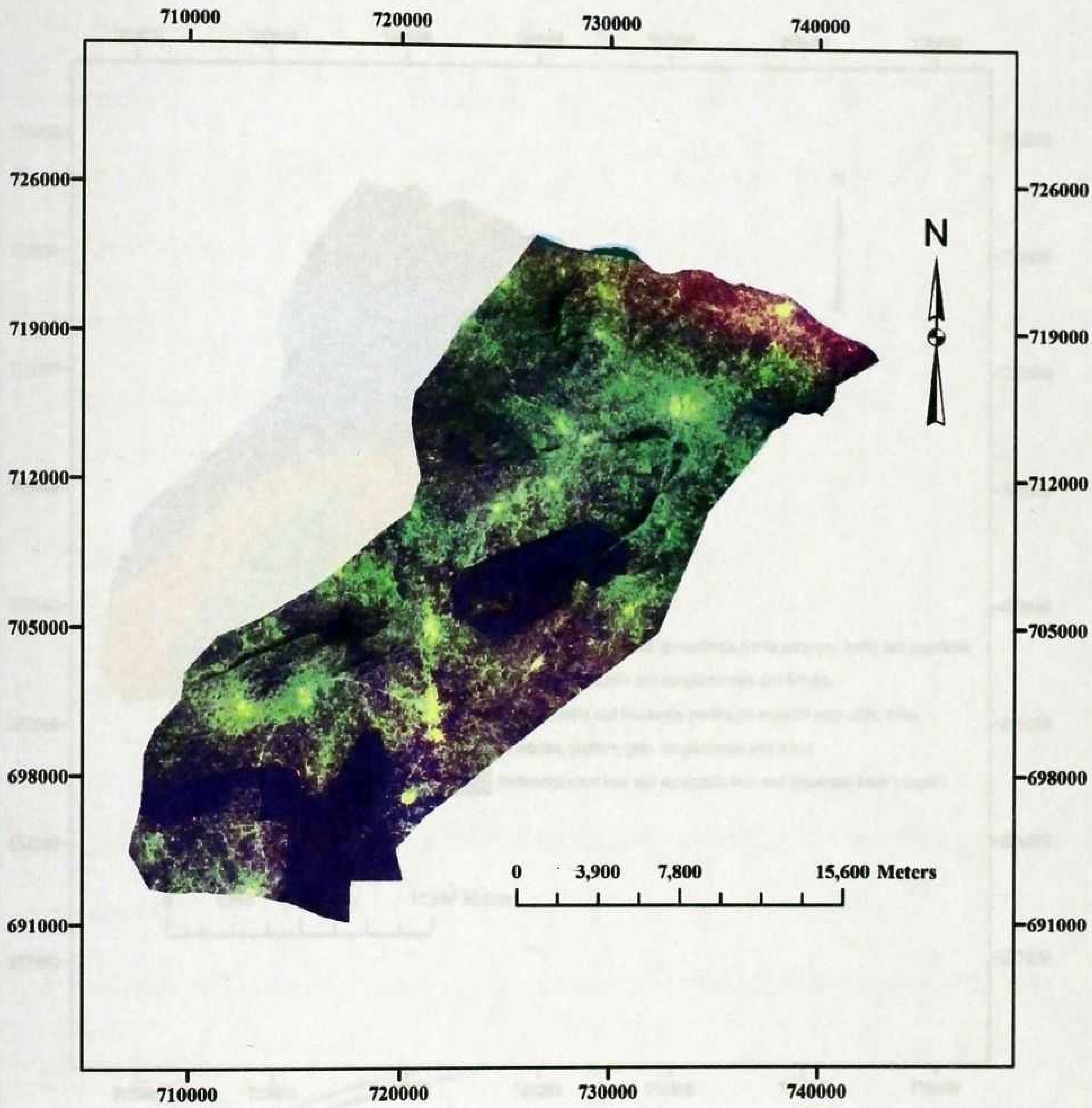

Figure 4.10: Result of the image composed of PC1, PC2 and PC3.

4.1.11 Result of Geologic Map of Birim North

The lithology or the various rock types within the study area are shown in the geologic map of Birim North and is displayed in Figure 4.11.

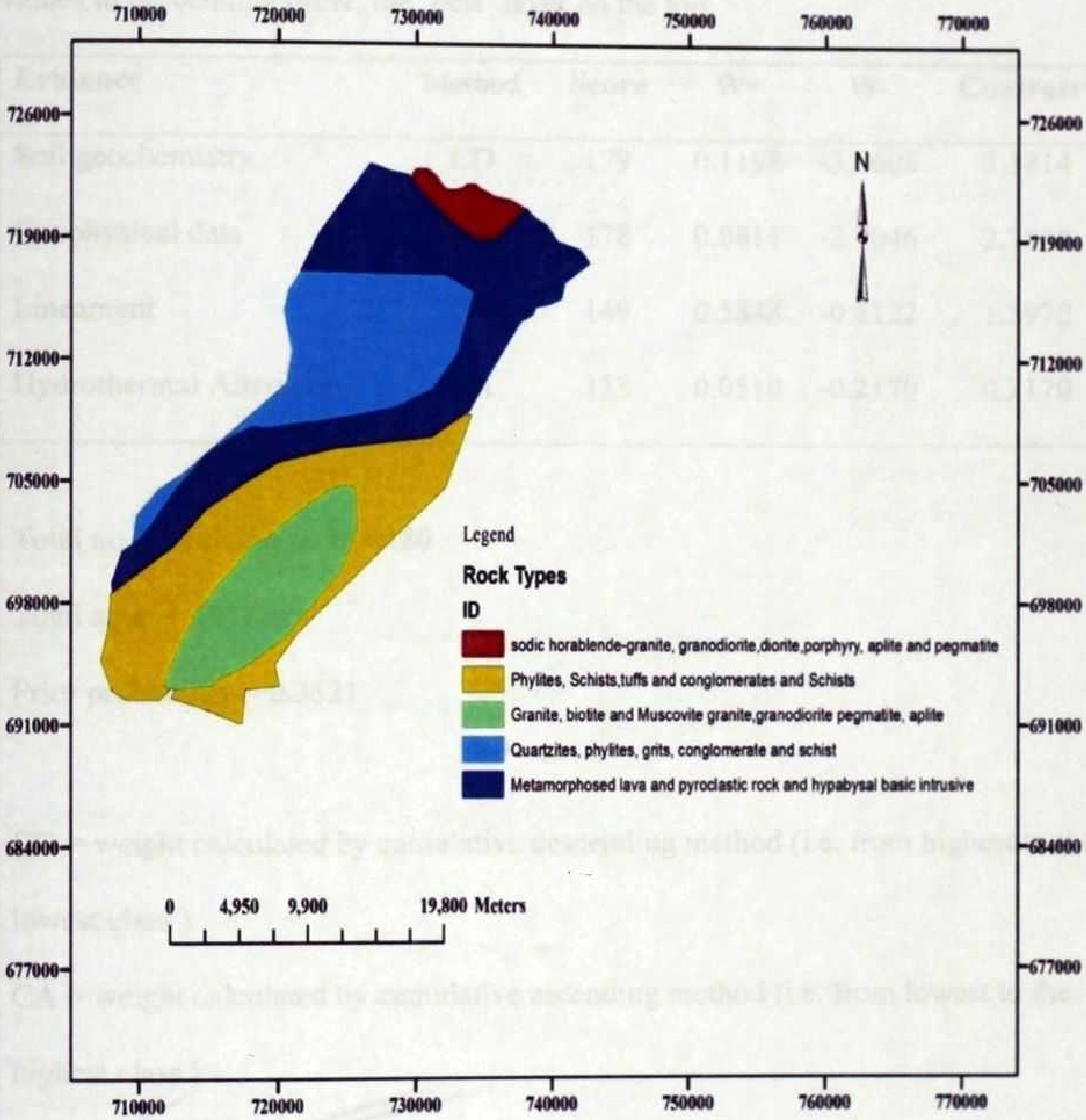

Figure 4.11: Geologic Map of Birim North.

Source: Ghana Geological Survey, 2005.

4.1.12 Result of Weights of Evidence

Table 4.1: Summary of the weights calculation. The evidence is sorted by contrast values in descending order, the 'best' layer on the top.

Evidence	Method	Score	W+	W-	Contrast*
Soil geochemistry	CD	179	0.1198	-3.0608	3.1814
Geophysical data	CA	178	0.0811	-2.7046	2.7858
Lineament	CA	149	0.5848	-0.8122	1.3970
Hydrothermal Alteration	CA	133	0.0510	-0.2170	0.2170

Total no. of training point =180

Total area = $497Km^2$

Prior probability = 0.3621

CD = weight calculated by cumulative descending method (i.e. from highest to the lowest class)

CA = weight calculated by cumulative ascending method (i.e. from lowest to the highest class)

Score = number of training point within the evidence

Contrast = W+ -W-

W+ = positive evidence

W- = negative evidence

4.1.13 Result of Gold Potential Map

The result of the gold potential map produced from this research work is displayed in the Figure 4.12.

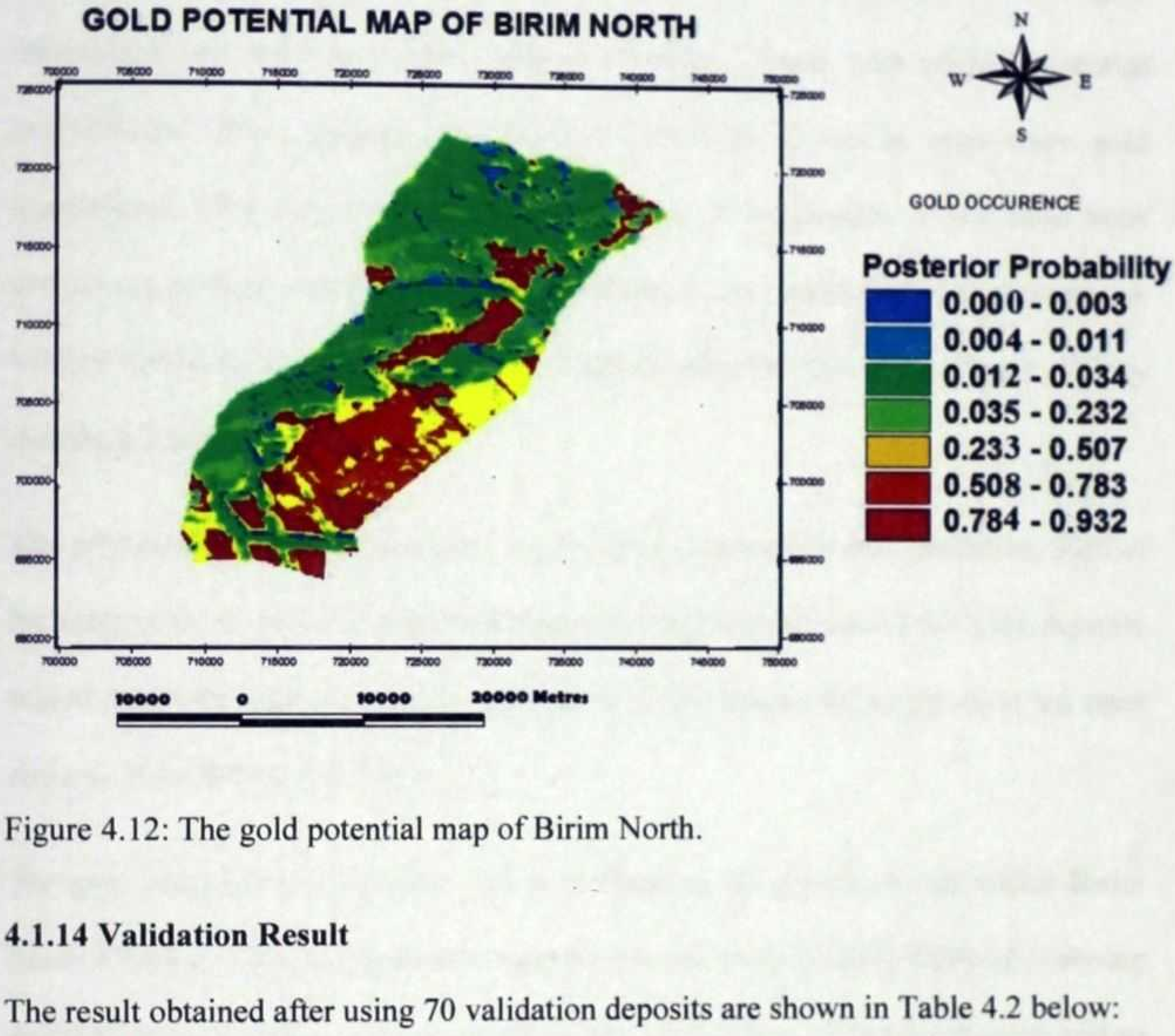

Figure 4.12: The gold potential map of Birim North.

4.1.14 Validation Result

The result obtained after using 70 validation deposits are shown in Table 4.2 below:

Table 4.2: The Validation Result.

Area	Posterior Probability	No. Of Validation Deposit	Percentage	Total Percentage
Unfavourable Areas	0.003 – 0.003	4 out of 70	6	17
	0.011 – 0.034	8 out 0f 70	11	
Favourable Areas	0.232 – 0.507	18 out of 70	26	83
	0.507 – 0.783	19 out of 70	27	
	0.783 -0.932	21 out of 70	30	

4.2 Discussion

It can be seen from Figure 4.12 that most gold occurring sites are within the areas with higher relative posterior probabilities. Locations with lower relative posterior probability values ranging from 0.003 to 0.232 can be considered as less gold mineralized and need no further exploration works. Areas with relative posterior probabilities values ranging from 0.232 to 0.932 are found to been more gold mineralized. This confirmed the fact that most of exploration works have been carried out at these areas. Also, Newmont Ghana Gold Limited-Akyem mine area is located within these higher relative probabilities areas as indicated in Figure 4.12 by the black border.

The gold potential map demarcates 158 km^2 as gold potential area, therefore, 32% of the total areas of 497 km^2 were favourable for the occurrences of the gold deposits within the study area. As a result, the area to be considered for exploration has been reduced from 497 km^2 to 158 km^2.

The gold potential map provides spatial information on gold resources within Birim North District. This information is essential in allowing District Mineral Planning Authorities to visualize the extent and spatial distribution of gold resources and to relate them to other forms of land use (such as urban areas or nature conservation areas) or to other factors (such as transport infrastructure and environmental information). With this gold potential map covering 32% of the whole of the district, the presence of a significant gold deposits have been known and can be considered when preparing land use plans. This prevent some land uses which are incompatible with future gold extraction. Also, the district could take a number of protective actions such as protection from galamsey operations provided the gold resources are not located in sites where gold extraction operations would conflict with existing urban uses or sensitive habitats. This map will intend assist in strategic decision making in respect of weighing the benefits of protecting sites for gold extraction against the benefits of developing these sites for alternative land uses.

The contrast gives unitless measure of the spatial correlation between gold occurrence and the evidential themes. From Table 4.1, all the evidential themes have a high relative contrast values greater than 1 except the hydrothermal alteration clay which has a value less than 1. The geochemical factor has the highest contrast value of 3.1814, followed by the geophysical factor with contrast value of 2.7858 and then the lineament factor of 1.3970. This means the best predictors of gold deposit in the study area are the geochemical factor, geophysical factor and the lineament. These evidential themes have higher relative contrast values and therefore, their present patterns are useful to recognize areas where gold deposits may occur. The geochemical data with the highest contrast value means that field prospecting is at least required when exploring new gold deposits.

The hydrothermal alteration clay has the least positive weight which is closer to zero and the lowest contrast value. Its present pattern is useful to recognize sites where gold deposits may not occur. This apparent poor association between the hydrothermal alteration clay and the gold deposit could be because (1) some areas mapped as alteration are probably unrelated to gold mineralization and (2) alteration halos around many small deposits are not large enough to be detected from Landsat image as indicated by Andrada-de-Palomera (2004). Also, Buckingham and Sober (1983) indicated that weathering processes can mask the spectral response of underlying rocks with coatings and internal mineralogical transformation since weathering processes produce the same mineral as hydrothermal alteration processes.

From Table 4.2, a total of 83 percent of the validation deposits fell within the predicted favourable gold areas or zones with posterior probability of 0.232 or higher while a total of 17 percent of the validation deposits or points also fell within the predicted unfavourable zones with posterior probability of less than 0.232. Therefore the gold potential model has a prediction rate of 83% (i.e, the percentage of the validation deposits or points in the predicted favourable gold deposits areas). The gold potential map also has a success rate of 88% (i.e, the percentage of the training deposits or points in the predicted favourable gold deposits zones) which correspond to 158 out of 180 training deposits that were used.

Figure 4.8 shows the lineament map of the Birim North District. The lineament, which are shorter in length indicate the form and position of individual folds, faults, joints, vein and lithologic contacts. These may lead to the location of gold deposit. These lineament reflect only immediate surface and near-surface conditions and are usually poor guide to concealed gold deposits. Linear features or lineament of greater length also indicate the general geometry of the folds, faults and other structures within the study area. These linear features are less abundant than the shorter linear features in terms of magnitude and are useful when defining the potential gold areas. Vassilas et al., (2002), used edge detection enhancement and on screen digitizing to extract lineament from satellite image. This means that using this approach can help extract lineament from satellite image.

Hydrothermal alteration clay can be mapped out by using the clay mineral index (band 5 to band 7). According to Jian and Philippa (2009), the clay minerals which are characteristic of hydrothermal alteration have strong absorption in the spectral range around 2.2μm corresponding to TM band 7 in contrast to high reflectance in the spectral range around 1.6μm corresponding to TM band 5.

The results in Figures 4.2, 4.3, 4.4 and 4.5 indicate the application of low pass operations on the band ratio image. The results from the low pass 7*7 kernel filters, low pass 5*5 kernel filters and low pass 3*3 kernel filter operations did not provide the best result as compared with the result obtained from the low pass 9*9 kernel filter operation. Therefore the low pass 9*9 kernel filter image was used in the production of the alteration map of Birim North to minimize the pepper-salt effect and high variability produced as a result of the band ratio.

As indicated by Rejash (2004), the delineation and characterization of hydrothermal alteration clay can be of great value in mineral exploration and assessment of new deposits as the spatial distribution of hydrothemally altered rocks is a key to locating the main outflow zones of hydrothermal system which may lead to the recognition of mineral deposits. From Figure 4.6, the areas with black colours show places where hydrothermal alteration has taken place and the white coloured areas are places where no alteration has occurred. Normally, the altered areas have the potential of being associated with gold minerization (Rejash, 2004).

From Figure 4.11, the various rock types within the study area are shown and this helps in identifying the rock types that are associated with gold mineralization. By comparing the gold potential map in Figure 4.12 and the geological map of Birim North in Figure 4.11, it can be seem that the rock types associated with gold mineralization are quartzes, phylites, schist, granites, conglomerate and biotite.

The principal component analysis in Figure 4.10 was a good way to find the different rock types as the analysis was able to separate the different rock types. However, some local information was needed in order to tell what each component is related to since the components do not carry out material information directly. The principal component analysis was only useful in identifying the various rock types within the study area rather than identifying altered rocks associated with gold mineralization.

Figure 4.9 shows the interpolation of the soil geochemical data by using the inverse distance weighting interpolator. The inverse distance weighting interpolator is a quick deterministic interpolator that is exact and helped in creating a spatial correlation between the sampled points taken and the gold content of those sampled points. Sampled points within the red coloured zone have the highest concentration of gold concentration, followed by sampled points within the yellowed coloured zone. Finally, those sampled points within the blue coloured zone have the least concentration of gold content.

CHAPTER FIVE

5.0 CONCLUSIONS AND RECOMMENDATION

5.1 Conclusion

The objective of this research work is to produce a gold potential map of Birim North District through the application of Remote Sensing and GIS. Based on the method used, the results obtained and the analysis of the results, the research has answered the following research questions:

5.1.1 How can gold potential areas in the Birim North be mapped out by using Remote Sensing and GIS?

This research work was able to produce the gold potential map of Birim North through the application of GIS and Remote Sensing technique by: (1) building a spatial digital database (2) extracting predictive evidence for a gold deposit (3) calculating weights for each predictive map (evidential theme) and (4) combining the evidential theme to predict the gold deposit.

The gold potential map also has a success rate of 88% (i.e, the percentage of the training deposits or points in the predicted favourable gold deposits zones) and a prediction rate of 83% (i.e, the percentage of the validation deposits or points in the predicted favourable gold deposits areas).

The integration of exploration datasets by using the Arc-weight of evidence is useful in the prediction of the possible gold potential areas within the study area and the integration process required less time and is less expensive.

5.1.2 What are the best predictors in the integration of the various exploratory dataset?

The best predicators that were used in the integration of the gold potential model are the geochemical factor, geophysical factor and the lineament. The alteration is the least predicator and the reasons are as follows: (1) some areas mapped as alteration are probably unrelated to gold mineralization (2) alteration halos around many small deposits are not large enough to be detected from Landsat image and (3) weathering processes can mask the spectral response of the underlying rocks with coating since weathering processes produce the same mineral as hydrothermal alteration processes..

5.1.3 What is the total area of gold mineralization within the study area?

The gold potential map demarcates 158 km^2 as gold potential area, therefore, 32% of the total areas of 497 km^2 were favourable for the occurences of the gold deposits within the study area. Areas with relative posterior probabilities between the values ranging from 0.232 and 0.932 are favourable gold potential areas.

5.1.5 What types of rock are associated with gold mineralization within the study area?

The rock types or the lithology associated gold mineralization within the study area are quartzes, phylites, schist, granites and biotite.

5.2 Recommendation

The research work recommends the following:

- The gold potential map produced from this research indicate that Remote Sensing and GIS can be used to explore gold deposit in more cost effective and efficient way and therefore it is recommended for use as a tool in the various mining companies in Ghana.

- Areas that are free of mineral rights and known to have higher relative posterior probabilities by the gold potential model should be considered for future exploration activities.
- Field verification must be done to determine the threshold value for generating the alteration

REFERENCES

Akhavi, M. S., and Raymond, D. A. (2001) RADARSAT-1 Imagery and GIS Modeling for Mineral Exploration in Nova Scotia, Canada, Geocarto International, v.16, Issue 1, pp.57-64.

Amer, R. M., Kusky, T. M., Ghulam, A. (2008) New Methods of Processing ASTER Data for Lithological Mapping: Examples from Fawakhir, Central Eastern Desert of Egypt, Journal of African Earth Sciences (in review).

Amos, B. J. and Geenbaum, D. (1989) Alteration detection using TM imagery: the effects of supergene weathering in arid climate. International Journal of Remote Sensing, v.10, pp.515-527.

Andrada-de Palomera, R. P. (2004) Application of Remote Sensing and GIS for Mineral Predictive Mapping, Deseado Massif, Southern Argentina, MSc. Dissertation, International Institute for Geo-information Science and Earth Observation, Enschede, The Netherland, pp.30-45, unpublished.

Apan, A., Kelly, R. Jensen, T., Butler, D., Strong, W. and Basnet, B. (2002) Spectral discrimination and separability analysis of agricultural crops and soil attributes using Aster imagery, Proc. of the 11th Australasian Remote Sensing and Photogrammetry Conf., Brisbane, Queensland, 2-6 September.

Asadi, H. H. (2000) The Zarshuran gold deposit model applied in a mineral exploration GIS in Iran, PhD Thesis, Delft University of Technology, Delft, The Netherlands, p.190.

Bennett, S. A., Atkinson, W. W. and Kruse, F. A. (1993) Use of Thematic Mapper imagery to identify mineralization in the Santa Teresa district, Sonora, Mexico. International Geology Review, v.35, pp.1009-1029.

Bennett, S. A., Atkinson, W. W., Jr., and Kruse, F. A. (1994) Use of Thematic Mapper imagery to identify mineralization in the Santa Teresa District, Sonora, Mexico: International Geology Reviews, V. 35, No. 11, pp. 1009-1029.

Birim North District Assembly (2006) District Medium Term Development Plan, an unpublished document.

Boleneus, D. E., Raines, G.L., Causey, J. D., Bookstorm, A. A., Frost, T. P., and Hyndman, P. C. (2001) Assessment method for epithermal gold deposits in Northeast Washington state using weight of evidence GIS modelling: US Geological Survey, Open-File Report 01-501, p.52.

Bonham-Carter, G. F. (1991) Integration of geoscientific data using GIS. In: Maguire, D. J., Goodchild, M. F., Rhind, D. W. (Eds.), Geographical Information Systems: Principles and Applications. Longman, Essex, pp. 171–184.

Bonham-Carter, G. F. (1994) GIS for geoscientists: Modelling with GIS, Pergamon, p.398.

Bonham-Carter, G. F., Agterberg, F. P., and Wright, D. F. (1988) Integration of geological datasets for gold exploration in Nova Scotia: Photogrammetry and Remote Sensing, 54, no.11, pp. 1585-1592.

Buckingham, W.F. and Sober, S.E. (1983) Mineralogical characterization of rock surfaces by hydrothermal alteration and weathering: Application to remote sensing. Economic Geology, v.78, pp.664-674.

Budkewitsch, P., Newton, G., and Hynes, A. J. (1994) Characterization and extraction of linear features from digital images: Canadian journal of Remote Sensing,v.20,p.268-279.

Burrough, P. A., and McDonnell, R. A. (1998) Principles of Geographical Information Systems. New York: Oxford University Press, pp. 23-34

Chandrasekar, N., Sheik Mujabar, P., and Rajamanckam, G., V. (2011) Investigation of heavy-mineral deposits using multispectral satellite data, International Journal of Remote Sensing, v.32, Issue 23, pp.8641-8655.

Chica-Olmo, M., Abarca, F., and Rigol, J. P. (2002) Development of a Decision Support System based on remote sensing and GIS techniques for gold-rich area identification in SE Spain, International Journal of Remote Sensing, v.23, Issue 22, pp. 4801-4814.

Crippen, R. E. (1989) Development of remote sensing techniques for the investigation of neotectonic activity, eastern Transverse Ranges and vicinity, southern California, Ph.D. thesis, Univ. of Calif., Santa Barbara, 304p., 1989b.

Crippen, R. E., Blom, R. G., and Heyada, J. R. (1988) Directed band ratioing for the retention of perceptually-independent topographic expression in chromaticity-enhanced imagery, International Journal of Remote Sensing, v.9, pp.749-765.

Crippen, R. E., Hajic, E. J., Estes, J. E. and Blom R. G. (1990) Statistical band and band-ratio selection to maximize spectral information in colour composite displays, International Journal of Remote Sensing, v.12, pp.567-572.

Ferrier, G., and Wadge, G. (1996) The application of imaging spectrometry data to mapping alteration zones associated with gold mineralization in southern Spain, International Journal of Rock Mechanics and Mining Sciences and Geomechanics Abstracts, 33(7), 308A–308A.

Fraser, S. J. (1991) Discrimination and identification of ferric oxides using satellite Thematic Mapper data: a Newman case study. International Journal of Remote Sensing, v.12, pp.635-641.

Fraser, S. J. and Green, A. A. (1987) A software defoliant for geological analysis of band ratios. International Journal of Remote Sensing, v.8, pp.525-532.

Gabr, S., Ghulam, A., and Kusky, T. (2010) Ore Geology Reviews, Elsevier, v.38, pp.59-69.

Gad, S., and Kusky, T. M. (2006) Lithological mapping in the Eastern Desert of Egypt, the Barramiya area, using Landsat thematic mapper (TM), Journal of African Earth Sciences, v. 44, pp.196–202.

Hongmei, W., Cuoray, C., and Qiumin, C. (2002) Data Integration Using Weights of Evidence Model: Applications in Mapping Mineral Resource Potentials. Paper presented at Symposium on Geospatial Theory, Processing and Applications: Ottawa, Canada, pp. 1-5.

Hunt, G. R. (1977) Spectral signatures of particulate minerals in the visible and near-infrared, Geophysics, v.42, 501-513.

Hunt, G. R. (1979) Near infrared (1.3-2.4μm) Spectra of alteration minerals-potential for use in remote sensing. Geophysics, v.44, pp.1974-1986.

Hunt, G. R. and Ashley, R. P. (1979) Spectra of altered rocks in the visible and near infrared. Geophysics, v.43, pp.602-607.

Jain, A K., (1989) Fundamentals of Digital Image Processing, Prentice Hall, Englewood Cliffs, NJ, p. 260.

Jian, G. L., and Philippa, J. M. (2009) Essential Image Processing and GIS for Remote Sensing: Algebraic operation (multi-image point operation). John Willey & Sons LTD, p.29.

Kaisser, H. S. S., Nashaat, S., Zahair, A. S., and Emad, S. (2004) Exploring gold occurrences in Wadi Alaqi District in Egypt using Remote Sensing and GIS technique, GISCO.

Karniel, A., Mesisels, A., Fisher, L. and Arkin, Y. (1996) Automatic extraction and evaluation of geological linear features from digital remote sensing data using a Hough transformation: Photogrammetric Engineering and Remote Sensing, v.62, p.525-531.

Katz, M. (1982) Lineament analysis of Landsat imagery applied to mineral exploration. In Mineral exploration techniques in tropical forest areas (Laming, D. I. C. and Gibbs, A. K. Eds).Hiden Wealth, pp.157-166.

Kaufman, H. (1988) Mineral exploration along the Aqaba-Levanat structure by use of TM data, concepts, processing and results. International Journal of Remote Sensing, v.9, pp.1630 -1658.

Kemp, L. D., Bonham-Carter, G. F., Raines, G. L. and Looney, C. G. (2001) Arc-SDM: Arcview extension for spatial data modelling using weights of evidence, logistic regression, fuzzy logic and neural network analysis. Ottawa, Canada. http://ntserv.gis.nrcan.gc.ca/sdm/ (Accessed on March. 20, 2012).

Kiafeng, Z., Micha, P., Nornan, D. (2007) Lithologic and Mineral Information extraction for gold exploration using Aster data in the South Chocolate Mountains (California). ISPRS Journal of Photogrammetry and Remote Sensing, Volume 62, Issue 4, September 2007, pp. 271-282.

Kruse, F. A. (1998) Advances in Hyperspectral Remote Sensing for Geologic Mapping and Exploration: in Proceedings 9th Australasian Remote Sensing Conference, Sydney, Australia, July 1998.

Kutina, J. (1969) Hydrothermal ore deposits in the western United States: a new concept of structural control of distribution. Science, v.165, pp.1113-1119.

Lahren, M. M., Schweickert, R. A. and Taranik, J. V. (1988) Analysis of the northern Sierra accreted terrain, California, with airborne thermal infrared multispectral scanner data. Geology, v.16, pp.525-528.

Legg, C. A. (1994) Remote Sensing and Geographic Information System: Geological mapping, mineral exploration and mining. John Willey & Sons and Praxis Publishing LTD, p.166.

Lepage, R., Rouhana, R. G., ST-Onge, B., Noumeir, R. and Desjardins, R. (2000) Cellular neural network for automated detection of geological lineaments on Radarsat image: IEEE Transactions on Geoscience and Remote Sensing, v.38, pp.1224-1233.

Liu, C. C., Sousa Jr., M. A. and Gopinath, T. R. (2000) Regional structural analysis by remote sensing for mineral exploration, Paraiba state, Northeast Brazil. Geocarto International, v.15, pp.69-75.

Loughlin, W. P. (1991) Principal component analysis for alteration mapping. Photogrammetric Engineering and Remote Sensing, v.57, pp.1163-1169

Madani, A. A., and Eman, A. A. (2009) SWIR ASTER band ratios for lithological mapping and mineral exploration: A case study from El Hudi area, South-eastern desert, Egypt, Saudi Society for Geoscience, pp.1-8.

Madina, A. A. (2001) Selection of the optimum Landsat Thematic Mapper bands for automatic lineaments extraction, Wadi Natash area, South Eastern Desert, Egypt. : 22nd Asian Conference on Remote Sensing, Singapore, 5-9 November 2001, 2001.

Mather, P. M. (1987) Computer Processing of Remotely Sensed Images, John Wiley & Sons, Chechester, England, p.328.

Nykänen, V. (2011) Prospectivity mapping in GIS: integrate geochemistry data with geophysics and geology. Workshop in the 25th International Applied Geochemistry Symposium 2011 22-26 August 2011 Rovaniemi, Finland. Vuorimiesyhdistys, B92-5, 88 pages.

O'Leary, D. W., Friedman, J. D., and Pohn, H. A. (1976) Lineament, linear and lineation: some proposed new standards for old terms. Geological Society of America Bulletin, v.87, pp.1463-1469.

Pirajno, F. (1992) Hydrothermal mineral deposits, Principles and fundamental concepts for the exploration geologists. Springer, Berlin.

Qihao, W. (2010) Remote Sensing and GIS Integration: Theories, Methods, and Application. The McGraw-Hill Companies, Inc. pp. 1-2.

Rajesh, H. M. (2004) Application of remote sensing and GIS in mineral resource mapping- An Overview, Journal of mineralogical and Petrological Sciences, v.99, pp.83-103.

Rein, B. and Kaufmann, H. (2003) Exploration for gold using panchromatic stereoscopic intelligence satellite photographs and Landsat TM data in the Hebei area, China. International Journal of Remote Sensing, v.24, pp.2427-2438.

Rokos, D., Mavrantza, R., Vamvoukakis, K., St-Seymour, Kouli, M., Karfakis, I. and Denes, G. (2000) Localisation of alteration zoning for the detection of epithermal gold by integration of remote sensing and geochemical techniques: Levas Island, Aegean, Hellas: Proceedings of the fourteenth International Conference on Applied Geologic remote Sensing, Las Vegas Nevada, pp.161-168.

Rowam, L. C., and Lathram, E. H. (1980) Mineral exploration, Chapter 17 in Remote Sensing in Geology (B. S. Siegal and A. R. Gilespie, editors).John Willey & Sons, New York, pp.553-605.

Ruiz-Armenta, J. R. and Prol-Ledesma, R. M. (1998) Techniques for enhancing the spectral response of hydrothermal alteration minerals in Thematic Mapper image of central Mexico. International Journal of Remote Sensing, v.19, pp.1981-2000.

Sabine, C., Realmuto, V. J. and Taranik, J. V. (1994) Quantitative estimation of granitoid composition from Thermal Infrared Multispectral Scanner (TIMS) data, Desolation Wilderness, northern Sierra Nevada, California. Journal of Geophysical Research, v.99, pp.4261-4271.

Sabins. F. F. (1999) Remote sensing for mineral exploration: Ore Geology Review, v.14. pp. 157-183.

Siegal, B. S. and Goetz, A. F. H. (1977) Effect of vegetation on rock and soil discrimination. Photogrammetric Engineering and Remote Sensing, v.43, pp.191-196.

Sijmons, k. (1987) Computer-assisted detection of linear features from digital remote sensing data, ITC J., 1987-1:23-31.

Smith, M. O., Johnston, P. E. and Adams, J. B. (1985) Quantitative determination of mineral types and abundances from reflectance spectra using principal component analysis. Journal of Geophysical Research, v.90, pp.797-804

Spatz, D. M. (1997) Remote sensing characteristics of the sediment and volcanic hosted precious metal system: imagery selection for exploration and developments. International Journal of Remote Sensing, v.18, pp.1413-1438.

Sultan, M., Arvidson, R., and Sturchio, N. C., (1986) Digital mapping of ophiolite melange zones from Landsat Thematic Mapper data in arid areas: Meatiq dome, Egypt, Geological Society of America Annual Meeting, Abstracts with Programs, v.18: p.766.

Suzen, M. L. and Toprak, V. (1998) Filtering of Satellite Images in Geological Lineament Analyses: An application to a Fault zone in Central Turkey.: International Journal of Remote Sensing, v.19, pp.1101-1114.

Tangestani, M. H. and Moore, F. (2001) Comparison of three principal component analysis techniques to porphyry copper alteration mapping: A case study, Meiduk area, Kerman, Iran. Canadian Journal of Remote Sensing, v.27, pp.176-182.

Tibaldi, A., and Ferrari, (1991) Multisource remotely sensed data, field checks and seismicity for the definition of active tectonics in Ecuadorian Andes, Int.J. Remote Sensing, v.12, pp.2344-2358.

Torres, C. A. (2007) Mineral Exploration Using GIS and processed ASTER Image, mini project, University of Texas at San Antonio, pp.1-16, unpublished.

Vassilas, N., Perantonis, S., Charous, E., Tsenoglou, T., Stefouli, M. and Varousfakis, S. (2002) Delineation of the lineaments from satellite data based on efficient neural network and pattern recognition techniques: Methods and Applications of Artificial Intelligence, second Hellenic Conference on Artificial Intelligence, SETN 2002, Proceedings, Thessaloniki, Greece, 2002, pp.355-366.

Washington Franca-Rocha, Bonham-Carter, G. and MISI, A. (2003) GIS Modeling for Mineral Potential Mapping of Carbonate-Hosted Pb-Zn Deposits, Revista Brasileira de Geociências, v.33, pp. 191-196.